76SRC39

NASA CR-145153

EXPLORATION OF AN OCULOMETER-BASED MODEL OF PILOT WORKLOAD

By

Marjorie J.Krebs

James W.Wingert

Thomas Cunningham

March 1977

Prepared under Contract No. NAS1-13092

By

Honeywell
SYSTEMS & RESEARCH CENTER
Minneapolis,Minnesota 55413

For

NASA
National Aeronautics and
Space Administration

1. Report No.	2. Government Accession No.	3. Recipient's Catalog No.
4. Title and Subtitle Exploration of an Oculometer-Based Model of Pilot Workload		5. Report Date March 1977 6. Performing Organization Code
7. Author(s) Marjorie J. Krebs, James W. Wingert, and Thomas Cunningham		8. Performing Organization Report No. 76SRC39 10. Work Unit No.
9. Performing Organization Name and Address Honeywell Inc. Systems & Research Center 2600 Ridgway Parkway Minneapolis, Minnesota 55413		11. Contract or Grant No. NAS 1-13092 13. Type of Report and Period Covered Contractor Report
12. Sponsoring Agency Name and Address National Aeronautics and Space Administration Washington, D.C. 20546		14. Sponsoring Agency Code
15. Supplementary Notes		

16. Abstract

The objective of the study was to investigate potential relationships between eye behavior and pilot workload. The work was performed by the Honeywell Research Center. A Honeywell Mark IIA oculometer was used to obtain the eye data in a fixed base transport aircraft simulation facility. The data were analyzed to determine those parameters of eye behavior which were related to changes in level of task difficulty of the simulated manual approach and landing on instruments. A number of trends and relationships between eye variables and pilot ratings were found. A preliminary equation was written based on the results of a stepwise linear regression. High variability in time spent on various instruments was related to differences in scanning strategy among pilots. A more detailed analysis of individual runs by individual pilots was performed to investigate the source of this variability more closely. Results indicated a high degree of intra-pilot variability in instrument scanning. No consistent workload related trends were found. Pupil diameter which had demonstrated a strong relationship to task difficulty was extensively re-examined. It was concluded that the generalized measure which showed this relationship was most likely not purely pupil diameter but a composite index incorporating the influence of other variables such as instrument scanning.

A separate but parallel analysis used Maximum Likelihood Estimation techniques with added oculometer information to identify dominant system variables being used as pilot inputs. The analysis, while limited in scope, was considered successful.

Recommendations for continued development of an oculometer related pilot model were provided.

17. Key Words (Suggested by Author(s))		18. Distribution Statement
Eye Movements Flight Simulators Pilot Ratings Workload Pilot Modeling	Maximum Likelihood Estimation	Unclassified - Unlimited

19. Security Classif. (of this report)	20. Security Classif. (of this page)	21. No. of Pages	22. Price*
UNCLASSIFIED	UNCLASSIFIED	118	$5.00

* For sale by the National Technical Information Service, Springfield, Virginia 22151

Page
Intentionally
Left Blank

TABLE OF CONTENTS

TABLE OF CONTENTS (Continued)

LIST OF ILLUSTRATIONS

LIST OF ILLUSTRATIONS (Continued)

LIST OF ILLUSTRATIONS (Continued)

LIST OF TABLES

LIST OF TABLES (concluded)

EXPLORATION OF AN OCULOMETER-BASED MODEL OF PILOT WORKLOAD

Marjorie J. Krebs, James W. Wingert, and Thomas Cunningham

Honeywell Inc.

Systems and Research Center

SECTION I

SUMMARY

This study was performed under contract number NAS 1-13092 sponsored by NASA Langley Research Center, Simulation and Human Factors Branch, from 29 April 1974 to 31 August 1976. The objective of the study was to investigate potential relationships between eye behavior and pilot workload. Ultimately, if stable relationships were found, the goal was to develop a predictive model usable in avionics display development programs. This model would be used for such applications as evaluating the suitability of instrument landing system equipment in providing a Category III landing capability for transport aircraft.

The work was performed by the Honeywell Research Center, Life Sciences Group. A Honeywell Mark IIA oculometer was used to obtain the eye data

in a fixed-base, transport aircraft simulation facility. The data were analyzed to determine those parameters of eye behavior which were related to changes in level of task difficulty of the simulated manual approach and landing on instruments. A number of trends and relationships between eye variables and pilot ratings were found. A preliminary equation was written based on the results of a stepwise linear regression. High variability in time spent on various instruments was related to differences in scanning strategy among pilots. A more detailed analysis of individual runs by individual pilots was performed to investigate the source of this variability more closely. Results indicated a high degree of intra-pilot variability in instrument scanning. No consistent workload-related trends were found. Pupil diameter which had demonstrated a strong relationship to task difficulty was extensively re-examined. It was concluded that the generalized measure which showed this relationship was most likely not purely pupil diameter but a composite index incorporating the influence of other variables such as instrument scanning.

A separate but parallel analysis used maximum likelihood estimation techniques with added oculometer information to identify dominant system variables being used as pilot inputs. The analysis, while limited in scope, was considered successful.

Recommendations for continued analysis of an oculometer-related pilot model were provided.

SECTION II

INTRODUCTION

As the difficulty of the piloting task increases due to adverse weather, aircraft stability changes, or a variety of other reasons, the pilot must work harder to maintain a constant level of performance. If the resulting workload is too high over too long a period of time, performance decrement will very likely result. Furthermore, the higher the workload under routine flying conditions, the less reserve the pilot has to draw upon if an emergency should occur. Clearly, it is desirable to find that workload level for the pilot which not only optimizes performance but also provides the extra capacity which may be needed only under certain critical conditions.

In considering alternative methods of measuring workload, it would be of value to have a tool with the additional advantage of providing diagnostic information as well. That is, it may not be enough to determine that one set of flight conditions has a higher workload level than another; the characteristics of the two conditions which contribute to workload differences could be critical. By having this additional diagnostic information, aircraft system designers would have an objective basis for eliminating or reducing potential problems for the pilot.

In the present study, the objective was to explore one such workload measurement technique. Scanning patterns and other eye behavior of pilots were recorded over a series of simulated aircraft approach and landing maneuvers. Task difficulty was increased by adding turbulence and

decreasing aircraft stability. The correspondence between changes in eye behavior and changes in task difficulty were then examined as the basis for formulating an initial model of visual workload.

The authors wish to express their appreciation to the following individuals for their many contributions during the course of this research program: Mr. Doug Engren of Western Airlines, the 737 pilot-consultant, whose extensive comments and suggestions during the development of the control station were invaluable; Mr. James Datta, who modified the simulation software extensively for purposes of this study; Mr. Richard Yenni, the Langley Research Center test pilot, who provided guidance in the modification of the simulation and Cooper-Harper ratings of the flight conditions which helped considerably in the analysis of the data; and finally, to Mr. Marvin Waller, Technical Monitor at Langley, for his guidance and cooperation during the entire program.

SECTION III

SUMMARY OF RESULTS

The major results obtained in the study are summarized below. More detailed information on each of these topics is provided in Section V.

INSTRUMENT DWELL TIMES

Very little change was found in average percent time spent on the various instruments as a function of task difficulty. Standard deviations reflected extremely large variability in the data. This variability was attributed to differences in scanning strategy for individual pilots. Analysis of variance performed on percent Attitude Direction Indicator (ADI) dwell time data showed no significant effects.

GENERAL EYE BEHAVIOR

Four other major variables not specifically related to the particular instrument set or flight conditions used in the study were investigated. These included: pupil diameter, blink rate, fixation duration, and saccade length. While the magnitude of the change in each of these variables as a function of flight segment and level of difficulty was small, each one showed a systematic relationship to the difficulty of the flying task. The change across flight segments was larger than that across difficulty levels.

WORKLOAD MODEL DEVELOPMENT

While trends were found in the data, variability was high. Stepwise linear regression analysis was explored as a means of expressing workload in eye behavior terms. Results indicated a strong relationship between Cooper-Harper ratings and general eye behavior. Pupil diameter changes provided the highest correlation with pilot ratings and accounted for 89 percent of the variance in the response variable. Correlations between pilot ratings and time spent on specific instruments were somewhat lower. The pupil diameter measure was subsequently analyzed in much greater detail. It was concluded that the measure used in the regression analysis was most likely not a pure index of pupil diameter but rather a composite measure reflecting both pupil dilation and scanning activity. It was further concluded that this in no way diminished its predictive value.

SYSTEM PERFORMANCE MEASURES

Three error measures were used to examine total system performance. These were RMS errors in glide slope, localizer, and approach speed control. When these measures were used to compare performance between the levels of difficulty, no statistically significant differences were found.

MAXIMUM LIKELIHOOD ESTIMATION

The use of maximum likelihood techniques to identify dominant pilot system variable inputs was considered successful. Although limited in scope, the analysis demonstrated the use of oculometer data as an input to the modeling process.

SECTION IV

METHODOLOGY

OVERVIEW

Data from a total of 200 runs for terminal approach and landing flight segments were collected in a fixed-base, six degree-of-freedom simulator. Eight experienced transport pilots from Northwest Airlines were used as subjects. Across runs, task difficulty was manipulated by varying aircraft stability and adding wind gusts to produce five levels of pilot workload. For each run, eye movement data were obtained using a Honeywell Mark IIA oculometer. System performance data were computed in the hybrid simulation. Eye data, control inputs, and system data were digitized on-line and recorded on magnetic tape for later analysis. A variety of plotting techniques and statistical analyses were used to evaluate the predictive capabilities of these variables in relation to pilot workload.

SIMULATION

All data were collected using the XDS Sigma Five Hybrid Computer to drive a simulated Boeing 737 aircraft. A general purpose aircraft six degree-of-freedom software package (GPASS) was used in the development of the simulation for this study. A description of the command laws and dynamics of the system are provided in Appendix A.

COCKPIT INSTRUMENTATION

The instrument set used in the study is shown in Figure 1. This set is comparable to presently installed instruments in commercial transport aircraft. This particular configuration of instruments was chosen to conform as closely as possible to a NASA/Langley Research Center simulation which is being used in other eye motion studies. This was the motivation for adding the two thin line meters around the ADI. The meter on the right side of the ADI displayed raw glide slope deviation. The meter immediately below the ADI displayed raw localizer deviation.

The instrumentation set was familiar to the subject pilots except for two features. The ADI had a speed command bug on the left side. This was an unfamiliar indicator to the pilots since it was not provided in the Boeing 727 which they were flying prior to this study. These pilots were accustomed to getting fast-slow information from the airspeed indicator. The vertical speed indicator consisted of a dial similar to a 737 instrument. This turned out to be slightly different from the one used in the 727 and caused a few problems in the training sessions for about half of the pilot subjects.

SIMULATED AIRCRAFT CONTROL STATION

One of the critical elements of any simulation from the standpoint of its impact on pilot performance is the control station. The force-feel system was similar in control motions and displacements to the 737, but the displacements, breakout forces, friction, force gradients, and fluid damping were all adjustable over a wide range. Pilots familiar with the 737 aircraft worked with the simulator development crew until acceptable parameters of the force-feel system were established by trial and error.

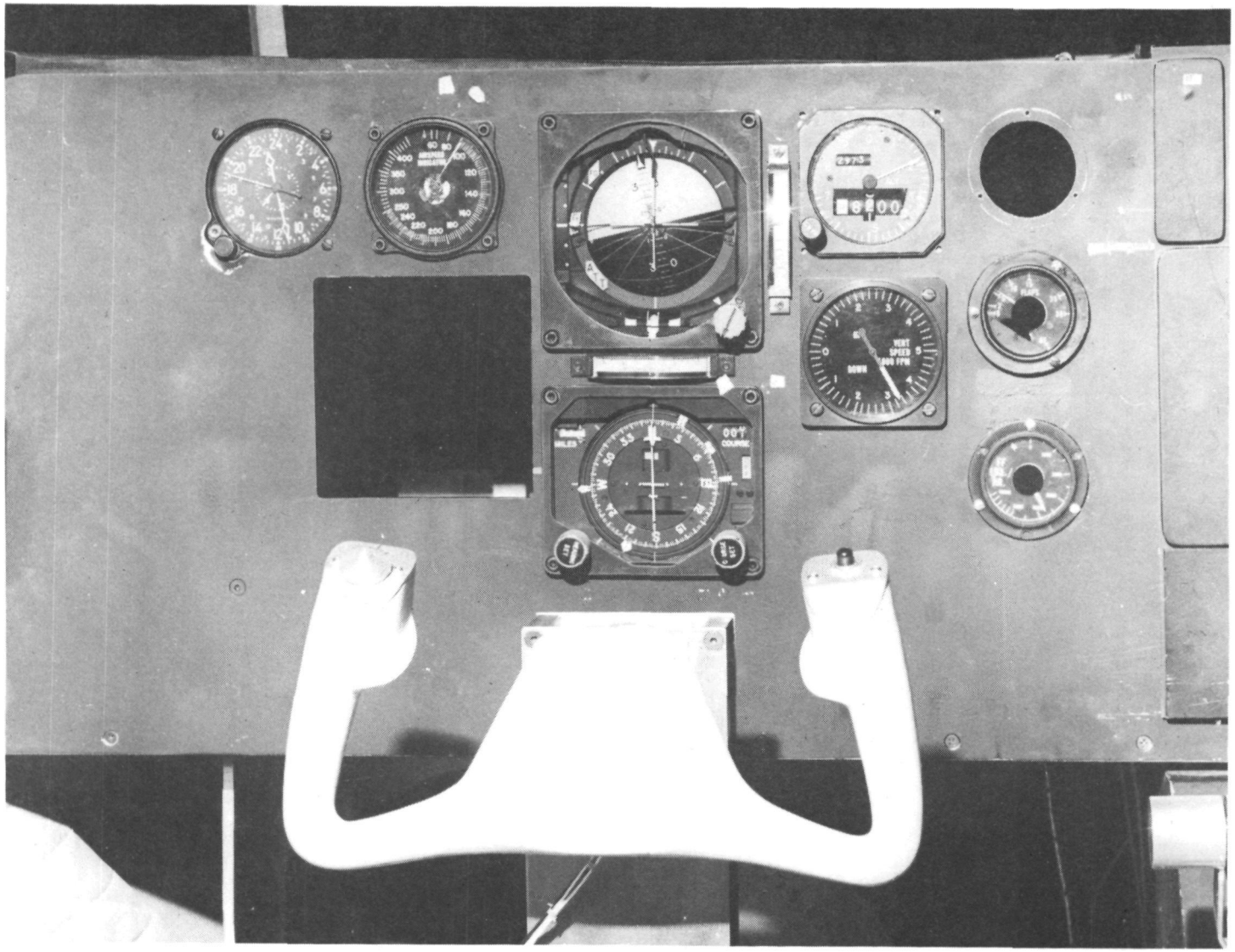

Figure 1. Instrumentation Set

EXPERIMENTAL VARIABLES

The difficulty of the flight control task was manipulated by varying vehicle stability and wind conditions. These were varied to obtain a wide range in the levels of task difficulty.

Two sets of vehicle stability models were developed. The first set was the baseline 737 vehicle model based on Boeing data. It was then varied as required until it was rated as nominally equivalent in handling characteristics to a Boeing 737 by two check pilots who were currently flying 737s.

In the preliminary simulator trials, it was evident that sufficiently difficult handling conditions could be generated with wind gust conditions to obtain data at the high end of the difficulty scale. Easy handling conditions were needed to obtain data at as low a level of difficulty as would be consistent with manual flight control conditions.

The easier handling conditions were generated by changing the stability augmentation system (SAS) parameters to obtain a more stable vehicle response. The autopilot gains changed were those that control the rate feedback components in the stabilization terms of both the lateral-directional and longitudinal axes of the aircraft. The roll axis SAS gain that is applied to the body rate gyro signal used for aileron damping was doubled. To increase this component of the pitch damping, the final pitch axis SAS gain that is applied to the pitch rate gyro signal was double the nominal value.

These magnitudes for the final stable vehicle gains were determined by applying two criteria:

- The pilot workload -- as measured by the secondary task workload technique -- was to be demonstrably lower with the stable vehicle.
- Pilot ratings of the stable vehicle handling qualities were to be favorable, with the vehicle as well damped as possible and still responsive to pilot inputs.

The wind model used in this simulation is based on a model recommended in Federal Aviation Regulations for the installation approval of automatic landing systems in transport category aircraft. This model is documented in FAA Advisory Circular 20-57A dated 12 January 1971.

The wind model used had two modes -- steady state and wind gusts. The steady state wind mode was entered as a headwind force. Initially the force vector was from 330° with respect to nominal heading (0° or north). The direction of force changed linearly as a function of altitude down to touchdown. At touchdown, direction was 30° with respect to nominal heading.

The wind gust model was computed as side and upward components. For up gusts a force vector component, W_g, was computed in body axes:

$$W_g = \frac{\sigma_w \sqrt{\frac{2V_x}{1750}}}{\frac{V_x}{1750} S + 1} W_r$$

where

σ_w = the magnitude of the standard deviation of wind gust magnitude selected for the trials by the experimenter

V_x = aircraft ground velocity

W_r = a program-generated random number between -1 and +1

S = the LaPlace operator

The magnitude of W_g corresponds to a 20-knot wind gust (3 σ value). For side gusts a force component V_g was computed in body axes:

$$V_g = \sigma_v \frac{\frac{2V_x}{1750}}{\frac{V_x}{1750} S + 1} V_r + V_{gnd} + V_h \cdot h$$

where

σ_v = the magnitude of the standard deviation of side wind gust value selected for the trials by the experimenter

V_x = aircraft ground velocity

V_r = a random number between -1 and +1

S = the LaPlace operator

V_{gnd} = magnitude of ground ride wind

V_h = altitude wind rate (m/sec/m)

h = altitude (meters)

The random number generator used was a model which approaches a Gaussian distribution with mean 0.0 and magnitude $\pm$ 1.0.

Gust values of 3 meters per second (1 sigma values) were used for both V_g and W_g. These are higher than expected values for turbulence but were established by test pilots in the pre-test phase. These values gave the appearance of moderate turbulence to the check pilots.

The magnitudes of V_g and W_g were chosen experimentally by pretrials using pilot subjects who would not participate in the main experiment. The selection criteria were:

1. Realism of the vehicle behavior, and
2. Range of empirically measured workload

In order to facilitate interpretation of the final data, it was desirable to maintain the piloting tasks as unchanged as possible throughout the changing levels. This eliminated the use of control system augmentation modes which would markedly reduce pilot workload but would also materially change the piloting taks, as would be the case with a completely automatic mode, for example.

Once an all-manual control mode decision was reached, the lowest possible level of difficulty was defined. It had to be the level obtained when the most stable vehicle model was used along with a no-disturbance or zero wind flight condition. The most difficult task was determined by making a number of simulation runs. This level was defined as the nominal vehicle plus wind condition which was marginally acceptable after the pilots were well-practiced. The intermediate levels were then determined by trial and error such that their workloads, as measured by the secondary workload task, would be regularly spaced.

SELECTION OF FLIGHT CONDITIONS

Five levels of task difficulty were selected based on the results of a preliminary test, using two pilots who would not be used in the main experiment. These conditions are defined in Table 1. The righthand column of that table provides a measure of workload for each condition as defined by the secondary

TABLE 1. DEFINITION OF FLIGHT CONDITIONS AND ESTIMATED WORKLOADS

Condition	Vehicle configuration	Wind	Workload (percent time required)
A	Stable	None	56
B	Stable	Gust 10	63
C	Nominal	None	69
D	Nominal	Steady state	74
E	Nominal	Gust 10	79

task. In the pretest, the secondary task consisted of two-digit numbers displayed on a nixie tube located at the extreme left of the instrument panel. The pilot was to add the two numbers and report the last digit of their sum. It was emphasized that performance on the primary flight task was to be maintained and that the secondary task was to be performed on a time-available basis only. By counting the average number of reported sums and estimating the time required for each one, total time spent on the secondary task could be calculated. Total run lenght minus time spent on the secondary task gave the time required by the primary flight task. This figure was converted to a p percentage for each condition and a workload metric was derived. Thus, the higher the number in the "Workload" column of Table 1, the higher the estimated workload for that condition. The five conditions defined in Table 1 and used in the main experiment were selected from a larger set of potential conditions. The criterion for selection was that the spread in calculated workload be maximized between pairs of conditions and over the entire set of five conditions.

It should be emphasized that the secondary task was used only during the pre-test. In the main experiment the pilot subject's only task was the flight task.

OCULOMETER

A Honeywell Mark IIa oculometer was used to record pilot eye data. It permitted head movement within a cubic foot* of space and tracked the eye up to ±40 degrees in the horizontal and +20 to -10 degrees in the vertical dimension. It had a measured accuracy across the field of view of approximatly ±1 degree over the effective range with greatest accuracy near the center. One degree is equivalent to about 2.5 cm. on the instrument panel.

Figure 2 shows the elements of the complete eye-motion recording system. It is composed of four major subsystems:

1. Oculometer - Picks up the image of the pilot's eye and outputs measures of eye pointing direction and pupil diameter.
2. Manual Control Station - Provides a manual control capability so that an operator can maintain the pilot's eye within the oculometer field of view.
3. Head Position Monitor - Shows the operator a view of the pilot subject's head to assist in reacquiring the pupil image in the event of head movement rapid enough to escape from the oculometer monitor.
4. Video Pointer Assembly - Combines the panel instrument image with a superimposed eye marker symbol to indicate the center of gaze of the pilot subject. The combination can be viewed during a flight and also videotaped for a permanent record.

* A cube approximately 30 cm per side.

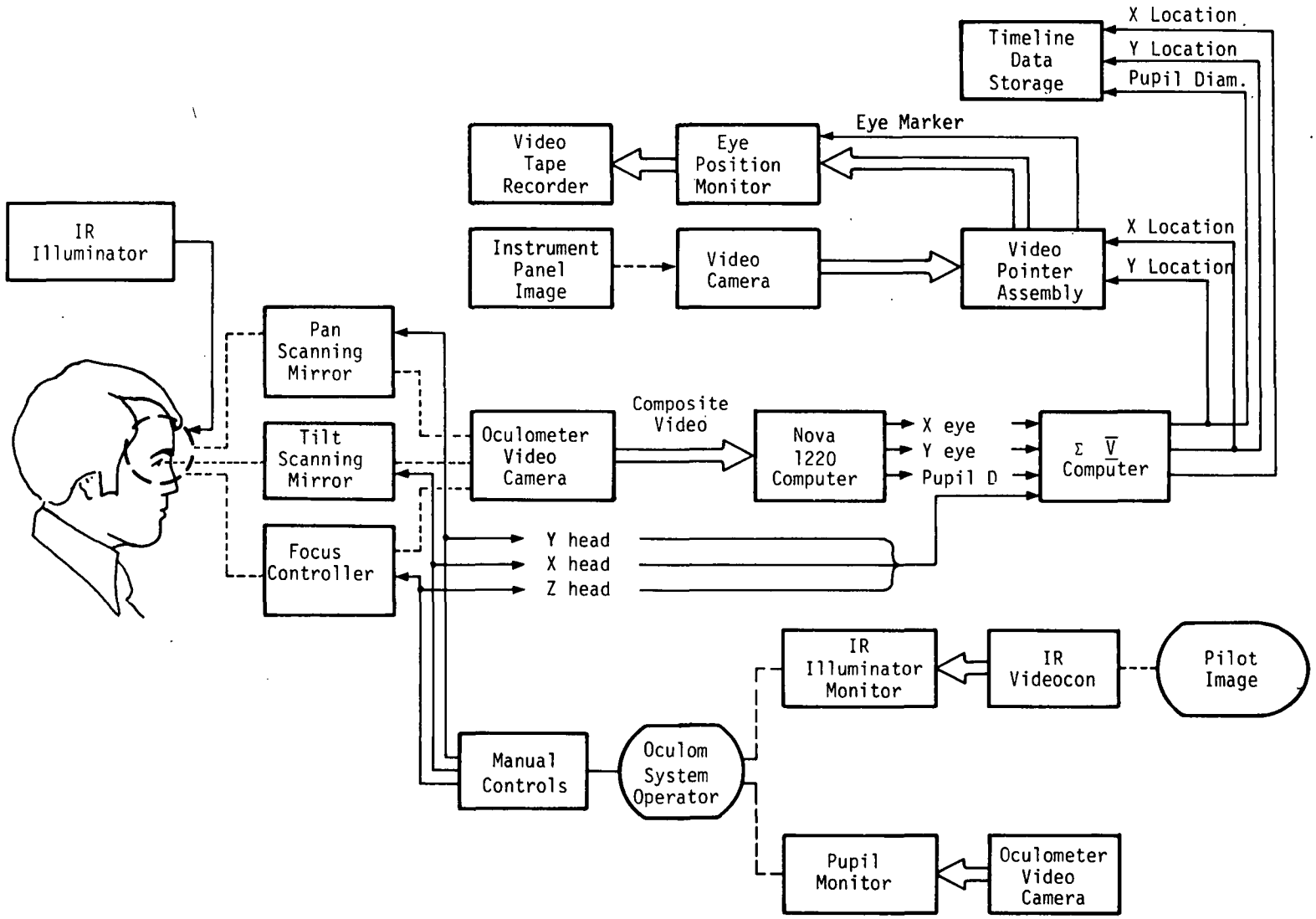

Figure 2. Functional Block Diagram of Mark IIa Oculometer

The oculometer was installed in the simulator cockpit with an in-line mounting in which the optical axis of the oculometer directly viewed the pilot's eye through a port in the instrument panel. Either eye of the pilot could be tracked. The oculometer was mounted in an adjustable bracket which allowed a gross adjustment to be made for eye height of the seated pilot.

RUN ORDER

A repeated measures design was used in the main experiment. All subjects were given five trials under each of the five conditions. The ordering of conditions within a block of five trials was counterbalanced across subjects and replications. See Table 2.

SUBJECTS

The eight subjects used in the main experiment were all Northwest Airlines copilots who were currently flying Boeing 727 commercial transport on a full-time basis.

TRAINING

The pilot subjects were trained by having them fly the same flight conditions that they would fly during the experiment. During the training exercises, the system performance variables were measured and recorded. After a block of runs was completed, the pilot subjects were given feedback of the performance scores recorded during those runs. Training continued until several criteria were met:

Table 2. Run Order Assignments

CONDITIONS TASK DIFFICULTY LEVEL	SUBJECTS							
	1	2	3	4	5	6	7	8
A	52134	56213	35124	25143	13425	53142	34512	24531
B	21453	14532	24315	54132	32154	43521	12354	42315
C	43521	32145	12543	41325	21453	25413	42351	51234
D	35412	51324	45321	13524	53421	31425	13145	14523
E	14235	24351	51342	35241	43512	15234	52413	31425

- The subjects had settled on a particular set of procedures to use for managing flaps, trim, and throttle and always repeated these procedures.

- Performance, defined by errors in glideslope, localizer and airspeed as used in the main experiment, had reached a plateau for a consecutive set of trial blocks.

- The pilot was satisfied that he understood the problems and could manage them.

DATA COLLECTED

The data recorded in the study are listed and described in Table 3. The parameters recorded are of a number of types. There are four whose purpose is to identify the data: tag, time, range to touchdown, and event line. The last needs more detailed description. The mission was broken up into segments or "events" which represented different piloting tasks and presumably different workloads. The five segments were:

Event 1 - Straight and Level Flight. Here the pilot task is to maintain a constant altitude while decelerating to final approach speed and holding ground track on localizer.

Event 2 - Glide Slope Acquisition. This is the transition period between level flight and constant descent.

Event 3 - Descent. This is a constant speed, constant flight path angle descent.

TABLE 3. DATA RECORDED

Parameter	Units	Description
Tag	------	Used to identify the data in each file by subject, replication, vehicle stability, wind and level
Time	Seconds	
Event line	Arbitrary	Used to identify the run segments
Glide slope	Radians	Raw data as displayed on the instrument
Localizer	Radians	Raw data as displayed on the instrument
Velocity	Knots	Raw data as displayed on the instrument
Altitude	Meters	Raw data as displayed on the instrument
Range	Meters	Calculated from stop end of runway
Horizontal pointer	Centimeters	Steering information as displayed on ADI
Vertical pointer	Centimeters	Steering information as displayed on ADI
Speed bug	Centimeters	Command information as displayed on ADI
Pitch	Radians	
Roll	Radians	
Heading	Radians	
Throttle	Kilograms	Thrust commanded
Stick F-A	Radians	Proportional to yoke fore-aft movement
Stick R-L	Radians	Proportional to yoke right-left movement
X-eye position	Centimeters	Horizontal position of eye relative to instrument panel
Y-eye position	Centimeters	Vertical position of the eye
Pupil diameter	Millivolts	Scale factor is 850 mV = 3 mm
Pen-Up	Volts	Level change indicates data loss

Event 4 - Preflare. This is the period just prior to flare, commencing at an altitude of 45.12 meters and ending when the flare command starts.

Event 5 - Touchdown. This segment includes flare and ends at touchdown.

Three major indicators of total system performance were recorded. These are the errors from nominal in glide slope, localizer, and velocity and were used as the criteria variables to characterize performance of the pilots on the five levels of difficulty.

SECTION V

RESULTS

OVERVIEW

Both system and eye analog data were sampled at a rate of 30 times per second, digitized, and placed on magnetic tape for later analysis. System data were analyzed to relate changes in performance to changes in task difficulty and to evaluate the difficulty index established in preliminary tests prior to the main experiment.

The eye data were analyzed to determine what, if any, systematic changes in eye behavior occurred as a function of task difficulty. The ultimate goal of this analysis was to define a set of eye behavior measures correlated with changes in pilot workload. These measures were then evaluated as to their applicability to a workload related model. Linear regression techniques were used to explore general trends in the data. Short-time history plots were used to examine individual run data in more detail. Finally, samples of data taken during prolonged dwells on the ADI were examined using maximum likelihood estimation techniques. The goal was to examine the value of this technique in determining what information the pilot was using when he looked at the composite flight director.

DATA REDUCTION

The series of x and y coordinates representing eye position were analyzed over time to determine when the subject dwelled (fixated) on some position

in the instrument array. A consecutive series of four x-y values which varied less than one degree from each other was defined as a minimum fixation time. Additional samples were added to a fixation until changes in the x-y values exceeded the one-degree limit. The number of samples contained in one of these fixations defined its duration. The average value of all the samples in the set determined its location. When a pair of x-y values exceeded the one-degree circle, it was counted as the beginning of an eye movement (saccade). A saccade continued until a new fixation was determined. The distance between two fixations defined the saccade length. This analysis, performed on the computer, was done for all samples of eye data across all 200 trials.

The fixation locations were then related to the specific flight instruments by defining the outer boundaries of each instrument and then counting any fixation within those boundaries as a dwell on that instrument. The number of samples contained in one fixation determined the fixation duration or dwell time. The sum of these over a specified interval was the total dwell time. In addition to instrument dwell time, fixation duration, saccade length, measures of pupil diameter, and blink rate were also obtained. For each run, a summary matrix of inter- and intra-instrument fixations was generated. This "fixation transition matrix" summarized the percentage of fixation shifts which resulted in either a change from one specified instrument to another or changes in fixation within the same instrument.

SYSTEM PERFORMANCE DATA ANALYSIS

The statistically analyzed system performance data parameters were the aircraft deviations from commanded profile:

glide slope errors (meters)

localizer errors (meters)

velocity errors (meters per second)

Each of these parameters was analyzed to determine if there were differences in performance on the individual conditions. This is important since performance can be traded off against workload. That is, if a condition is more difficult to control, the pilot can accept greater error and still have about the same workload as in an easier condition where error is lower.

System performance was compared between levels to determine if there were different accuracies obtained for the differing task difficulties. When the subjects are pooled, only small differences in mean error result. Error data for Event 3, the descent segment, are presented in Table 4.

Table 4. Means of Error Data for Event 3, the Descent Segment (Standard Deviations in Parentheses)

	CONDITION				
	A	B	C	D	E
Glide Slope Error (meters)	23.85 (13.05)	22.23 (10.10)	23.58 (12.57)	16.78 (10.23)	25.47 (12.17)
Localizer Error (meters)	4.03 (1.04)	3.81 (1.13)	5.40 (1.22)	5.40 (1.65)	4.85 (1.13)
Speed Error (meters per sec)	2.90 (1.71)	2.84 (1.86)	2.96 (1.77)	2.87 (1.60)	2.53 (1.80)

Individual comparisons of these error data by subject and level of difficulty were made using the Tukey Test. This method was selected from among several which have been developed to minimize errors when a large number of repeated comparisons are made. It has been established that wrong decisions owing to type 1 error are probable when testing repeatedly at a fixed α level.

A number of statistical researchers have developed methods for constructing simultaneous confidence intervals which avoid the pitfall of permitting the type 1 error to become excessively large. These methods basically depend on the use of a statistic calculated from the range of the means of the comparisons to be made, rather than using all the treatment means (as in the F tests). This kind of technique is more appropriate to the present data because the data distributions tend to pile up at certain values rather than distribute across the range. The statistic calculated is:

$$q = \frac{\bar{X}_{\text{highest}} - \bar{X}_{\text{lowest}}}{\sqrt{\text{Mean Square Error}/n}} \qquad (1)$$

The classic method (Newman-Keuls) prescribes a critical value for the difference between two means that depends on the number of ordinal steps between the two means being compared. The Neuman-Keuls procedure was modified by Tukey to use a single critical value for all comparisons, rather than adjusting the critical value depending on the number of steps between the treatment means being compared. This approach is more conservative in keeping the type 1 error small because it uses the critical value for the maximum number of steps for all comparisons. This critical value is, therefore, the largest criterion number to satisfy. This assures that the procedure has the property that all tests performed on differences between pairs of means have a level of significance which is at most equal to α.

The results of the Tukey tests for individual comparisons were not statistically significant at the $\alpha = 0.05$ level. There are not, therefore, consistent degradations of performance in the more difficult flight conditions. This indicates that pilot workload must be increasing in the harder flight conditions to compensate for the increasing difficulty of the control task.

Analysis of Vehicle-Related Data

As indicated above, pilot performance,in terms of absolute error of deviation scores, did not change significantly across levels of difficulty. While overall error was not statistically different across levels, the amount of change reflected in the instruments and pilot control maneuvers required to maintain performance errors at a fairly constant level varied widely. In Table 5, the computed rate of change of seven state variables and three control input variables are presented as a function of task difficulty. The first two columns, HSP and VSP, represent rate of change of the horizontal and vertical command bars of the ADI. Theunits are centimeters/second. Airspeed (SPD) variability is in meters/second. Pitch, roll and heading are in radians/second and altitude (ALT) is in meters/second. The three control movements are throttle (kilograms/second), stick movement fore and aft (radians/second) and stick movement right and left (radians/second).

Table 5 shows that the change rates are not ordered according to the preassigned ordering of levels of task difficulty. In fact, if the data are reordered as follows: A, C, D, B, E from "easy" to "difficult", almost all of the state and control variable values in the table are also ordered from low to high. Figures 3, 4 and 5 show six of the variables from Table 5.

Table 5. RMS Rate of Change as a Function of Task Difficulty for Seven State Variables and Three Control Inputs

CONDITION	HSP cm/ sec	VSP cm/ sec	SPD meters/ sec	PITCH rad/ sec	ROLL rad/ sec	HEAD rad/ sec	ALT meters/ sec	THROT. kg/hr/ sec	STICK F-A rad/ sec	STICK R-L rad/ sec
A	0.77	0.36	0.20	.00	.01	.01	0.17	15.62	.65	.28
B	1.35	0.54	0.28	.00	.01	.02	0.23	22.71	.92	.41
C	1.00	0.42	0.20	.00	.01	.01	0.21	15.98	.66	.30
D	0.88	0.46	0.23	.00	.01	.01	0.06	17.10	.70	.31
E	1.57	0.64	0.31	.01	.02	.02	0.24	25.37	.91	.42

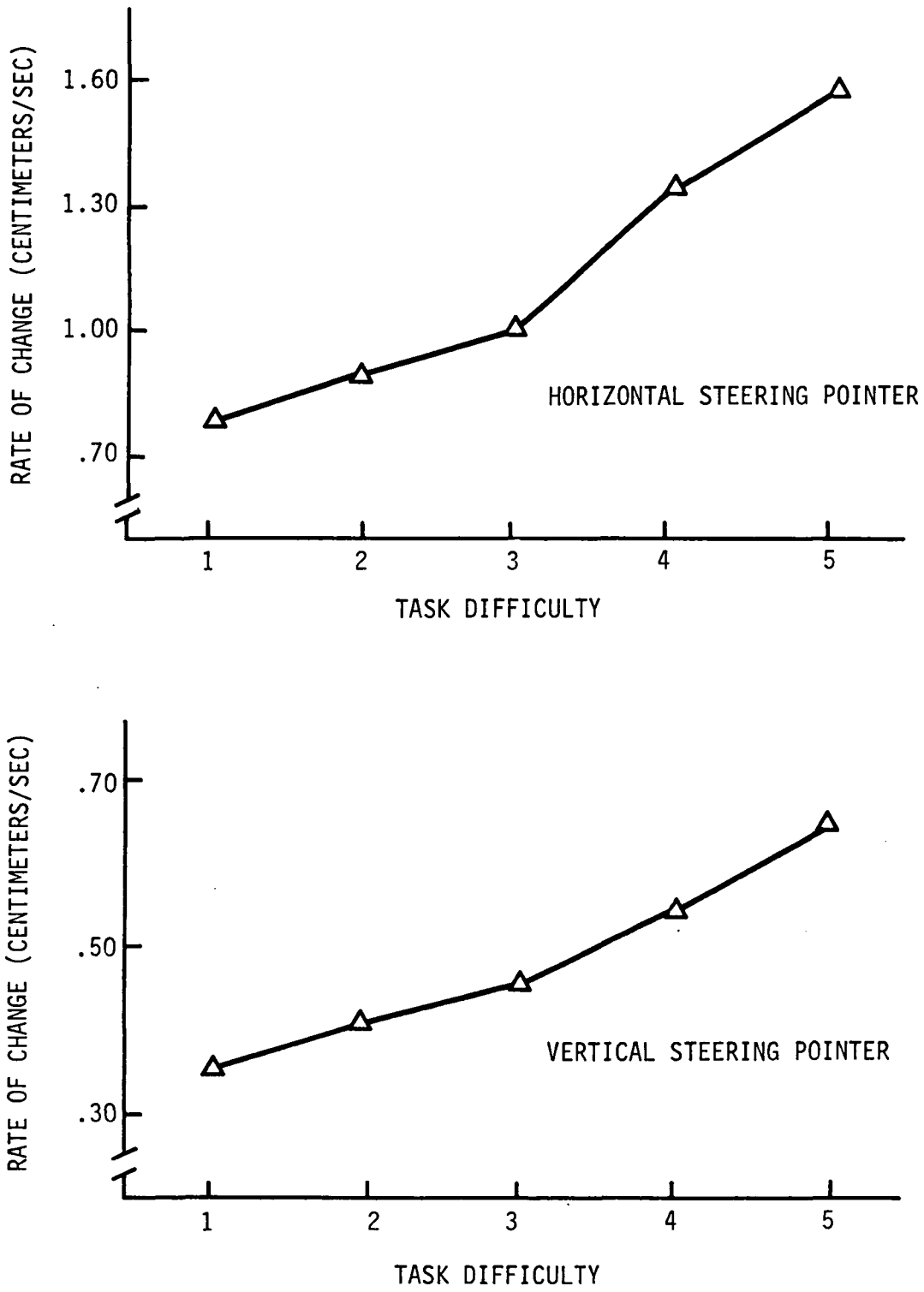

Figure 3. Rate of Change of the Horizontal (Top) and Vertical (Bottom) Steering Pointers of the ADI as a Function of Reordered Task Difficulties

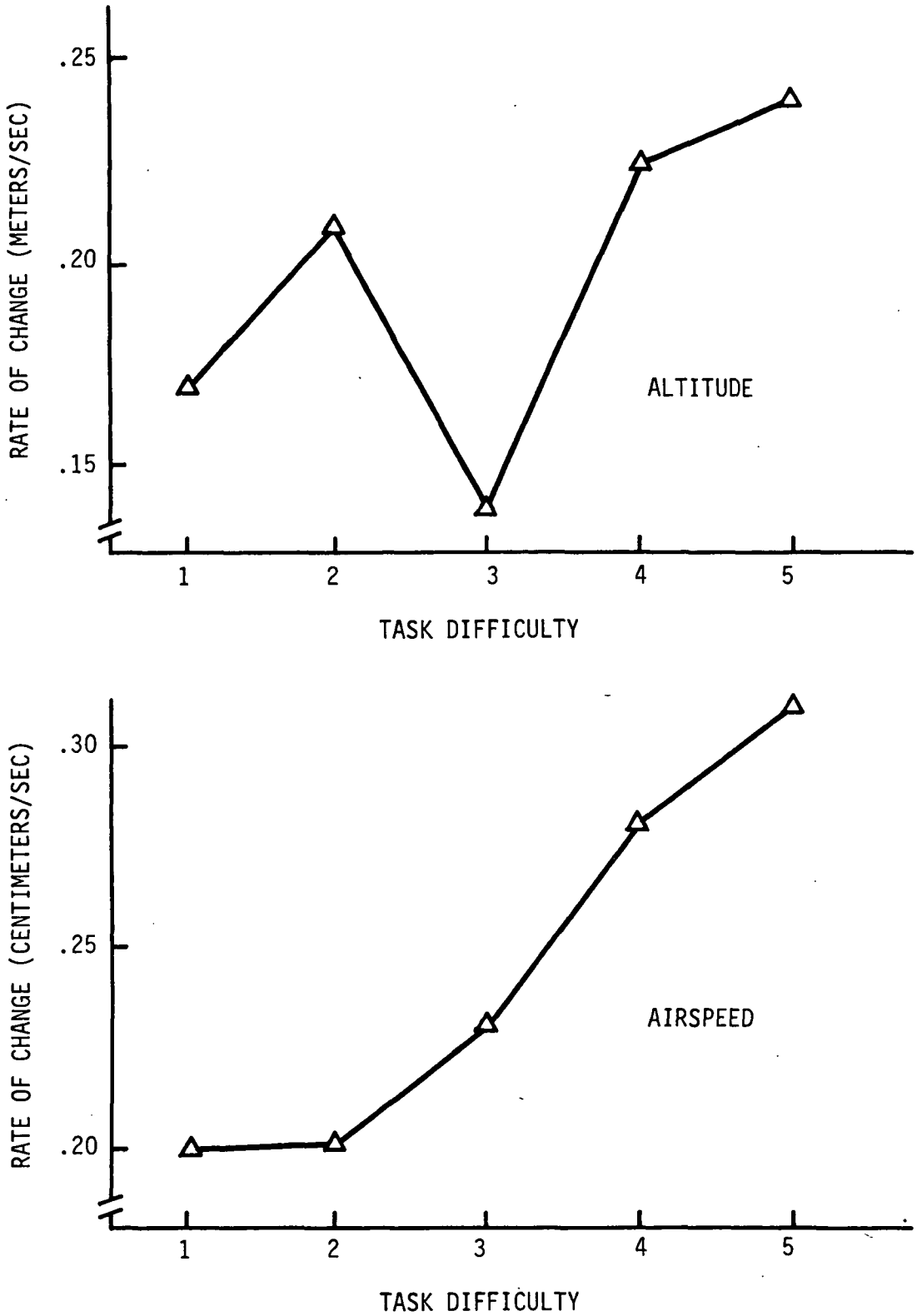

Figure 4. Rate of Change in Altitude (Top) and Airspeed (Bottom) as a Function of Reordered Task Difficulties

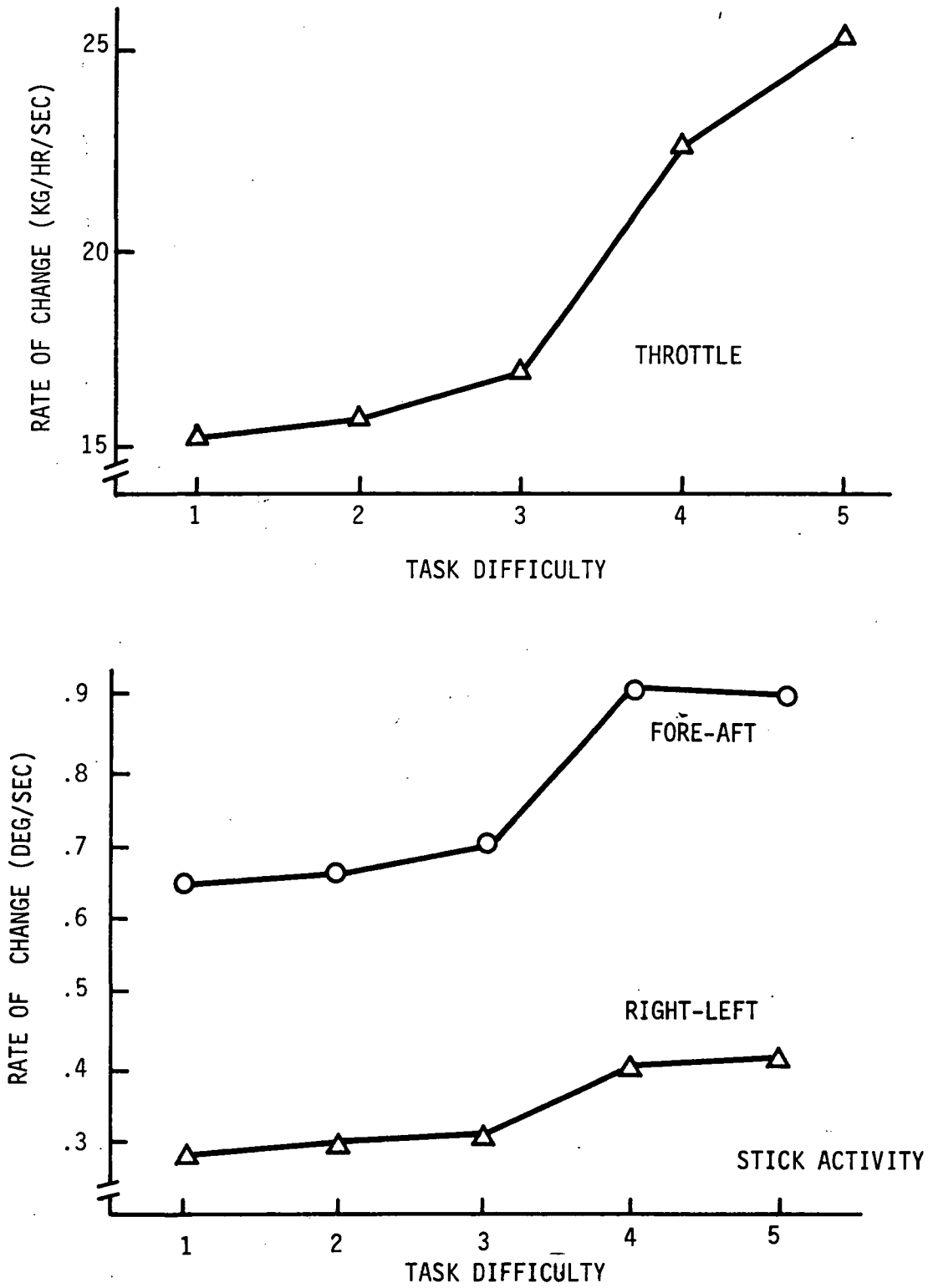

Figure 5. Rate of Change in Throttle (Top) and Stick Activity (Bottom) as a Function of Reordered Task Difficulties

A test pilot from Langley Research Center provided Cooper-Harper ratings (Appendix B) for each of the five conditions. Table 6 shows that these ratings are perfectly correlated with reordered difficulty levels shown in Table 5. The intervals between the Cooper-Harper ratings provided by the NASA test pilot were also highly predictive, particularly the relative similarity between conditions A, C, and D. Figure 5 clearly shows this for pilot control movements.

Table 6. Comparison of Cooper-Harper Ratings of NASA Pilot and Reordered Task Difficulties

Task Destination	Cooper-Harper Rating	Difficulty Level
A	3.0	1.0
B	5.5	4.0
C	3.5	2.0
D	4.0	3.0
E	7.0	5.0

Task Difficulty and Pilot Workload Redefined

The above findings for the system data indicate that the preliminary ordering of levels of task difficulty using the secondary task method was not predictive of the ordering obtained in the main experiment. Since all of the system variables and the pilot control inputs are ordered in a way perfectly correlated with the Cooper-Harper ratings, this latter measure was chosen as the index of pilot workload. The experimental data discussed below are interpreted using the reordered task difficulty levels as indicated in Table 6.

Analysis of Oculometer Data

The oculometer data were examined in two different ways. First, general trends were investigated using linear regression techniques. For this purpose, data were averaged over each run for each of the variables of interest. Following this general analysis, individual runs by individual pilots were examined in

much greater detail. The primary oculometer variables investigated were:

1) Average dwell time (fixation duration)
2) Total dwell time on each instrument (per run)
3) Saccade length
4) Blink rate
5) Pupil diameter

LINEAR REGRESSION ANALYSES

In an attempt to build a preliminary model of visual workload, all of the eye variables listed above were analyzed using stepwise linear regression techniques. In the regression analysis the correlation between changes in task difficulty and the set of performance measures was computed. If the correlations between task difficulty and some subset of performance measures were strong enough, the output of the analysis would be an expression of the relationship between the two. Ideally, the relationship is descriptive because it accounts for a large percent of the total variability obtained in the experiment and thus be highly descriptive.

The results of this analysis are shown in Table 7, a correlation matrix showing the relationship between eye variables and pilot rating, and in Table 8, a summary of the stepwise linear regression analysis. Variables 4 through 15 in the correlation matrix represent percent total dwell time on the specific instrument. The correlation matrix indicates that the oculometer variable with the highest correlation with the predictor variable was pupil diameter (0.94), followed by saccade length (0.88) and percent total ADI dwell time (0.79). The remaining variables had moderate to low correlations with pilot rating.

Table 7. Correlation Matrix for All Eye Variables Entered into the Regression Analysis. The Bottom Row of This Table Indicates the Correlation of Each of these Variables with the Predictor Variable: Pilot Rating.

VARIABLES	CORRELATION															
1. Pupil Diameter	1.000	.436	.921	.110	.570	.294	.602	.469	.448	.364	.458	.499	.183	.320	.858	.944
2. Fixation Duration	.436	1.000	.445	.034	.214	.105	.354	.178	.165	.123	.175	.205	.050	.097	.400	.440
3. Saccade Length	.921	.445	1.000	.199	.650	.314	.507	.479	.468	.441	.544	.573	.179	.343	.768	.880
4. Clock	.110	.034	.199	1.000	.222	.014	.089	.024	.029	.150	.058	.056	.000	.041	.025	.116
5. Airspeed	.570	.214	.650	.222	1.000	.169	.427	.292	.230	.174	.255	.341	.060	.138	.354	.541
6. Bank	.294	.105	.314	.014	.169	1.000	.067	.241	.031	.040	.131	.102	.263	.174	.264	.258
7. Speed Bug	.602	.354	.507	.089	.427	.067	1.000	.192	.217	.123	.097	.250	.008	.040	.243	.624
8. Glideslope	.469	.178	.479	.024	.292	.241	.192	1.000	.116	.117	.386	.278	.120	.080	.410	.413
9. Localizer	.448	.165	.468	.029	.230	.031	.217	.116	1.000	.441	.146	.346	.013	.203	.213	.469
10. HSI	.364	.123	.441	.150	.174	.040	.123	.117	.441	1.000	.163	.344	.018	.169	.163	.382
11. Altimeter	.458	.175	.544	.058	.255	.131	.097	.386	.146	.163	1.000	.344	.133	.219	.439	.412
12. VSI	.499	.205	.573	.056	.341	.102	.250	.278	.346	.344	.344	1.000	.093	.179	.336	.464
13. Flaps	.183	.050	.179	.000	.060	.263	.008	.120	.013	.018	.133	.093	1.000	.115	.186	.165
14. Fuel	.320	.097	.343	.041	.138	.174	.040	.080	.203	.169	.219	.179	.115	1.000	.294	.262
15. ADI	.858	.400	.768	.025	.354	.264	.243	.410	.213	.163	.439	.336	.186	.294	1.000	.793
16. Pilot Rating	.944	.440	.880	.116	.541	.258	.624	.413	.469	.382	.412	.464	.165	.262	.793	1.000

Table 8 shows that pupil diameter alone accounts for 89 percent of the variance in pilot rating as indicated by the R^2 value. The remaining variables when combined with pupil diameter contribute little to the predictive power. Saccade length drops out of the list of variables because of its high correlation (0.92) with pupil diameter.

This relationship can be expressed in the following equation:

$$\text{Workload} = 2.34 \times \text{pupil diameter} \qquad (2)$$

where workload is the value of the Cooper-Harper pilot rating for that condition and pupil diameter is in millimeters.

While pupil diameter was initially considered to have some potential in its relationship to pilot workload, the fact that none of the other variables entered into the equation was surprising. Therefore, each of the oculometer-based measures was examined in more detail.

INSTRUMENT DWELL TIMES

The percent of the total dwell time spent on each of the ten major instruments was computed by subject for each level of task difficulty. These data were then pooled across subjects to obtain an overall average percent total dwell time per instrument for each of the five difficulty levels. The results are presented in Table 9 together with the associated standard deviations. The average values in Table 9 show trends for the ADI and VSI but the remaining instruments show no consistent increase or decrease. The most striking feature in this table is the magnitude of the standard deviations. In many cases, they are several times larger than their corresponding means.

Table 8. Summary Table of Stepwise Linear Regression Analysis Showing the Sequence in Which Variables Were Entered, R^2 (the Percent of Variance Accounted for), and Increase in R^2 (the Increase in Predictability Achieved with the Addition of a Given Variable).

Step Number	Variable Entered	Variable Removed	Multiple R	Multiple R^2	Increase In R^2
1	Pupil Diameter	-	.9436	.8903	.8903
2	Speed Bug	-	.9461	.8952	.0043
3	Localizer	-	.9479	.8985	.0033
4	ADI	-	.9500	.9024	.0040
5	HSI	-	.9526	.9075	.0050
6	Airspeed	-	.9536	.9094	.0019
7	Bank	-	.9540	.9102	.0008
8	Altimeter	-	.9544	.9109	.0007
9	Flaps	-	.9547	.9115	.0006
10	Fuel	-	.9549	.9118	.0003
11	Clock	-	.9551	.9121	.0003
12	VSI	-	.9551	.9123	.0002
13	Glideslope	-	.9551	.9123	.0000
14	Fixation Duration	-	.9551	.9123	.0000

Table 9. Average Percent Total Time Spent Fixating for Each Instrument by Level of Task Difficulty. Standard Deviations in Parentheses.

	INSTRUMENT									
TASK DIFFI-CULTY	CLOCK	ASP	GSL	LOC	HSI	ALT	VSI	FLAPS	FUEL	ADI
Level 1	.05 (.20)	6.24 (6.92)	1.05 (2.57)	7.45 (13.15)	3.50 (6.94)	2.05 (4.07)	4.30 (8.14)	.04 (.21)	.36 (1.03)	74.95 (58.44)
Level 2	.09 (.38)	7.82 (13.09)	.88 (1.27)	6.49 (11.73)	2.81 (4.24)	2.46 (5.40)	3.39 (4.12)	.07 (.51)	.30 (.89)	75.69 (61.54)
Level 3	.32 (2.57)	5.45 (7.04)	.79 (1.61)	8.58 (15.05)	5.33 (13.06)	1.95 (3.62)	3.09 (3.18)	.08 (.45)	.49 (1.54)	73.93 (63.22)
Level 4	.12 (.65)	5.39 (6.47)	1.06 (1.80)	7.42 (13.01)	3.48 (7.68)	1.91 (2.90)	3.06 (6.31)	.12 (.41)	.29 (.85)	77.14 (64.89)
Level 5	.22 (1.59)	5.70 (7.31)	.67 (1.34)	9.37 (18.06)	5.80 (14.61)	1.49 (2.96)	2.36 (3.17)	.13 (.95)	.15 (.43)	74.10 (68.54)

Prior to performing an analysis of variance on the dwell time data, each of the columns in Table 9 was tested for homogeneity of variance using Cochran's test (Reference 5, Myers, 1966). This statistic uses the ratio of the sums of the variances for a given set of data to the maximum variance from that set. The obtained value is then compared to a critical value. If the critical value is exceeded, the variances are not homogeneous and a critical assumption of the F-test is violated. The results of that analysis indicated that of the data for the ten instruments, only the ADI data demonstrated homogeneity of variance. An analysis of variance was computed for these data and a summary of that analysis is provided in Table 10. Neither the two main effects (level and replication) nor their interaction was significant.

One possible reason for the lack of significant trends and also the high variability discussed above is that individual pilots had different scanning strategies. It was also possible that these individual strategies might reflect some consistent effects produced by increasing task difficulty. In order to investigate this possibility, each of the 200 runs was examined in detail, looking for a relationship between instrument scanning and workload.[2]

Several methods were used to examine the individual run data. First, averaged data for each run by each subject was examined. Second, short time history plots were prepared for each of the 200 runs. These plots, generated on the computer, were examined to search for clues concerning what changes, if any, occurred in pilot scanning as task difficulty increased. An example of one series of plots is provided in Figures 6a, 6b, 6c, and 6d. The size of

---

[2] The subjects were very similar in background. There was no available evidence suggesting that one or more could be classified as either substantially more or less experienced than the others.

Table 10. Summary Table, Analysis of Variance* for the Percent Total Time Spent on the ADI as a Function of Task Difficulty

Source	SS	df	MS	F
Total	85379.00	199		
Level (L)	242.95	4	60.74	0.47 --
Replication (R)	1675.11	4	418.78	1.19 --
RxL	589.48	16	36.84	0.54 --
Subjects (S)	61642.14	7	8806.02	
SxL	3655.68	28	130.56	
SxR	9874.76	29	352.67	
SxRxL (Residual)	7698.88	112	68.74	-- Non Significant

*The model used for this analysis was the repeated measures, randomized blocks design as discussed in Myers (Reference 5, 1966, pg. 156). In the non-additive model assumed here, the appropriate F-ratios were constructed as follows:

$$MS_L / MS_{SxL}$$

$$MS_R / MS_{SxR}$$

$$MS_{RxL} / MS_{SxRxL}$$

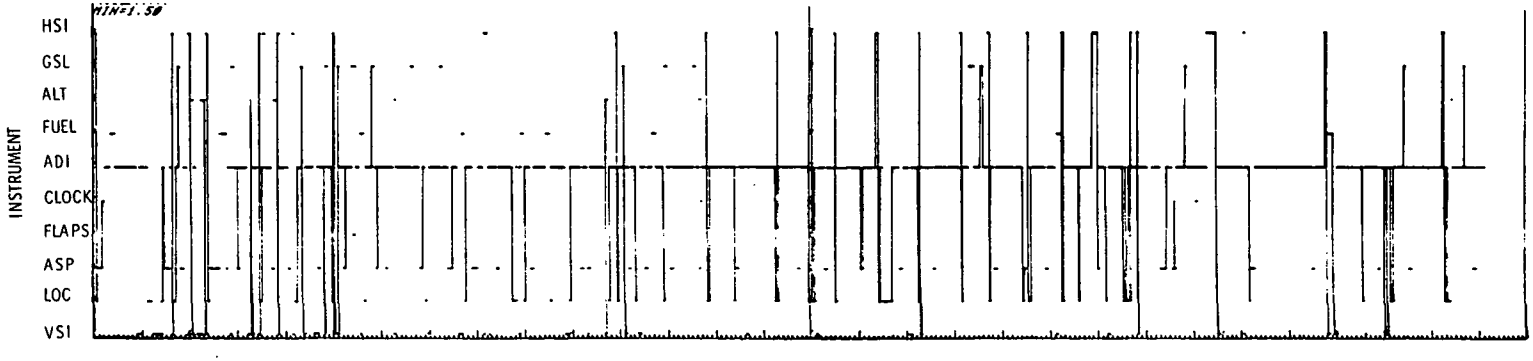

Figure 6a. Instrument Fixations, Subject 1, Difficulty Level 1, Replication 5

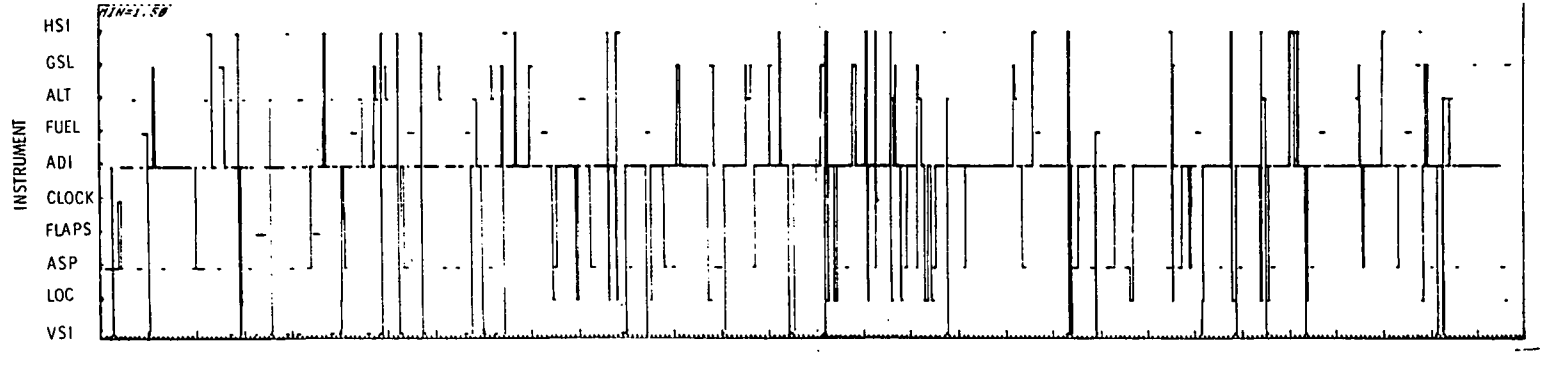

Figure 6b. Instrument Fixations, Subject 1, Difficulty Level 3, Replication 1

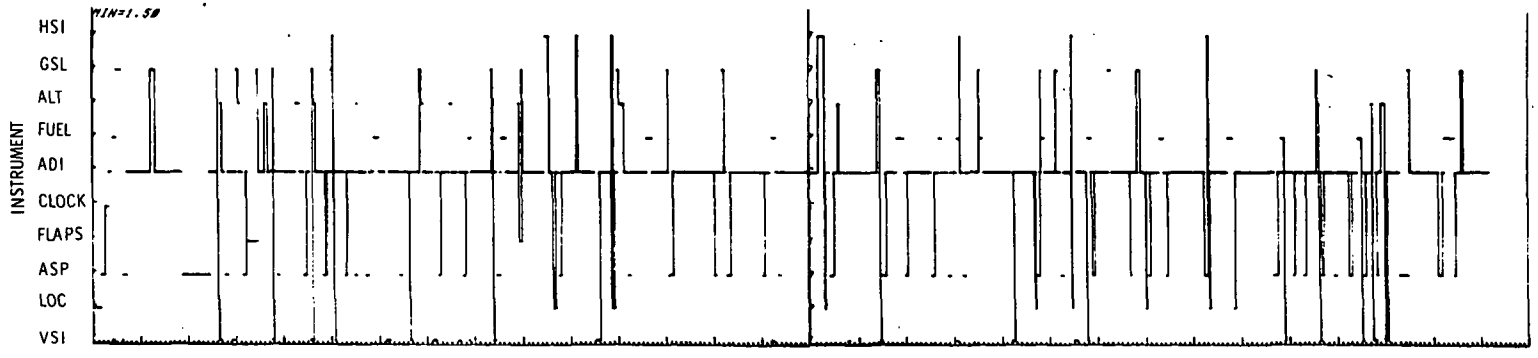

Figure 6c. Instrument Fixations, Subject 1, Difficulty Level 5, Replication 1

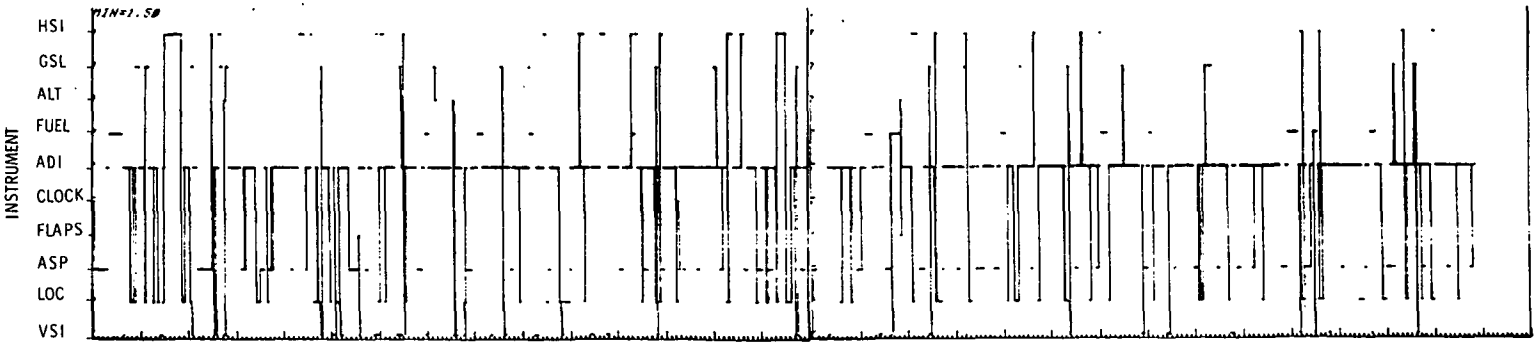

Figure 6d. Instrument Fixations, Subject 1, Difficulty Level 5, Replication 5

each plot is greatly reduced from the original. The ten instruments are represented on the ordinate and dwells on these instruments are plotted as a function of time into run; thus both frequency and duration information is available. It would be prohibitive in terms of space to attempt to reproduce all of these plots and would add little information to this report; however, it can be stated that differences were difficult to quantify. What was seen was a difference in the overall pattern of the line structure in the plot. In addition to differences among pilots, there were also differences observed within a pilot over several replications of the same difficulty level (see Figure 6a, 6b, 6c, and 6d). That is, a consistent pattern representative of one pilot or one group of pilots was not found.

The variability seen in the plots was explored further by looking at examples of inter- and intra-subject data. In Figure 7, the average number of dwells on the ADI is plotted as a function of task difficulty for six subjects. Both the group mean and individual data are shown. While the group mean tends to rise slightly as task difficulty increases, individual data show different trends. Data for Subjects 2 and 6 show a decrease in number of dwells on the ADI; for Subject 4, an increase; and for Subject 1, no consistent trend. Thus the group trend is not generally representative of the individual means. Similar results were obtained for other members of the instrument set.

As a final attempt to discover a consistent relationship between instrument scanning and task difficulty, a series of stepwise linear regressions analyses were run on subsets of the data. Each run was divided into eight to ten 30-second segments (depending on run length). Averages were obtained for each segment for each instrument for the following variables:

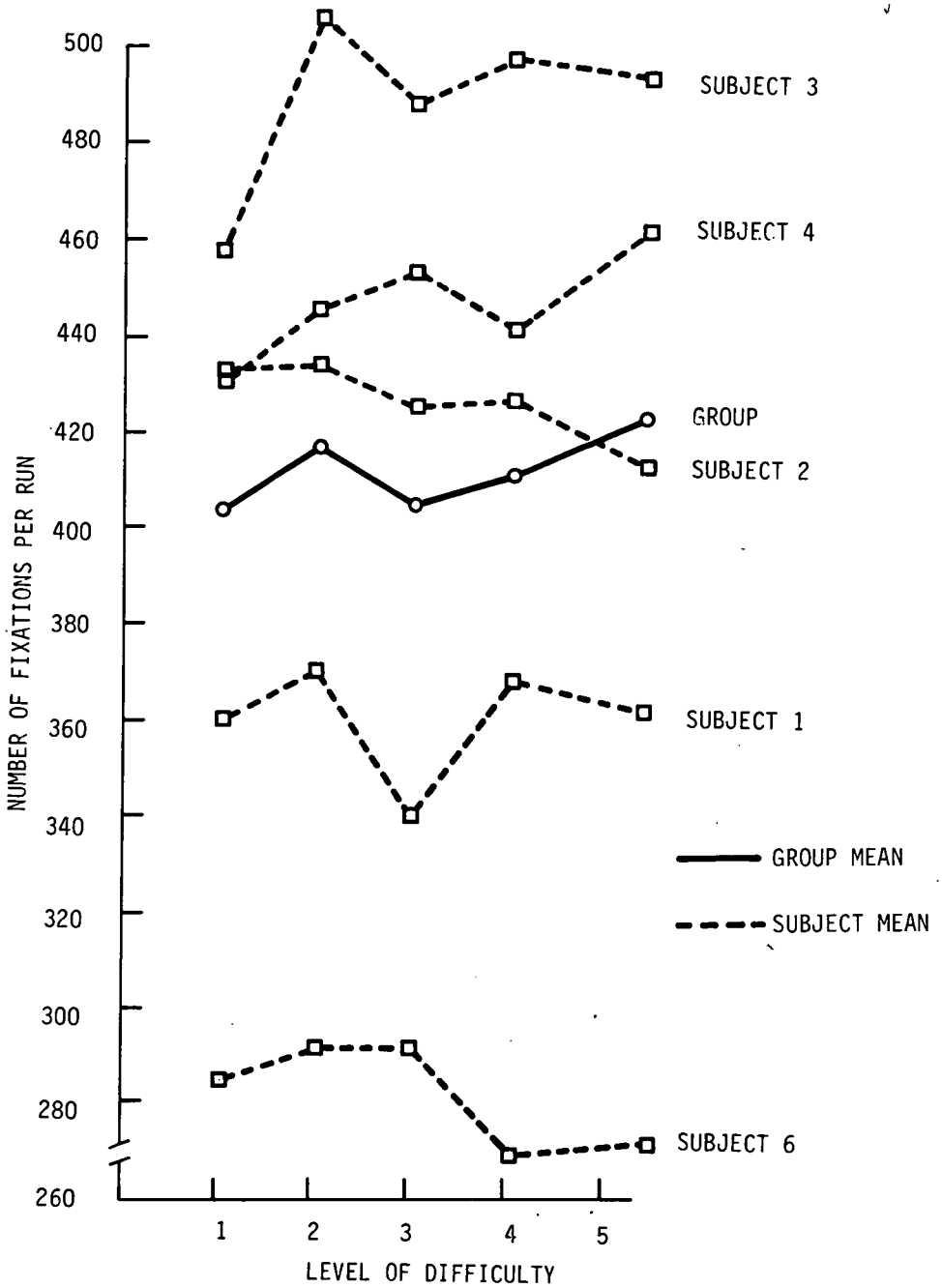

Figure 7. Number of Fixations per Run on the ADI, Individual and Group Means

1) Number of looks

2) Average dwell time

3) Total dwell time

Regression analyses were then run for all subjects, for individual subjects, and for all subjects pooled over selected time segments (for example, the last 90 seconds before touchdown). In all cases, the response variable was the Cooper-Harper rating. In all, about 30 such analyses were performed. None, however, yielded total R^2 values above 0.35 and most were considerably below that value, even when all variables were forced into the equation. At least as far as the present data set is concerned, it must be concluded that no relationship has been found between instrument scanning activities and pilot workload.

Average values on a number of other eye-related variables were obtained for each subject on each run. It was later decided that the averages over an entire four or five minute trial were not discriminating across some of the variables; therefore, each run was further divided into five segments as follows:

Event 1 - Straight and level flight

Event 2 - Glideslope acquisition

Event 3 - Descent

Event 4 - Preflare

Event 5 - Touchdown

Of these five Events, only 1, 3, and 5 proved to be useful, since glideslope acquisition and preflare lasted only a few seconds -- an interval too short

to meaningfully express data in percentages. Therefore, most of the data in the following section are presented as averages over the entire run, or averages for Events 1, 3, and 5. Data from Events 2 and 4, representing less than two percent of the total, have not been used.

SACCADE LENGTH

Under higher workload levels, it was hypothesized that a subject might tend to "lock on" to an individual instrument or he might develop an erratic scan pattern. Either of these, if they were to occur, would be reflected in the average saccade length or interfixation distance.

An erratic scan pattern would likely lead to longer average saccade lengths. On the other hand, if the pilot were to focus heavily on one instrument or several central instruments, it would lead to much shorter average distances. The average saccade lengths for individual subjects by event and level are presented in Table 11 and Figure 8. There is a slight but consistent decrease in length of eye movement across levels and a slightly larger decrease across events. In fact, comparisons across events within subjects showed that 86 percent of the saccade lengths decreased from Event 1 to Event 3 and Event 3 to Event 5.

SACCADE LENGTH VERSUS INSTRUMENT SCANNING

It was obvious from studying the instrument scan data averaged across subjects that variability was much too high to make generalizations. Therefore, a more detailed analysis of one individual subject was performed to help clarify some of the potential relationships. In particular, the relationship

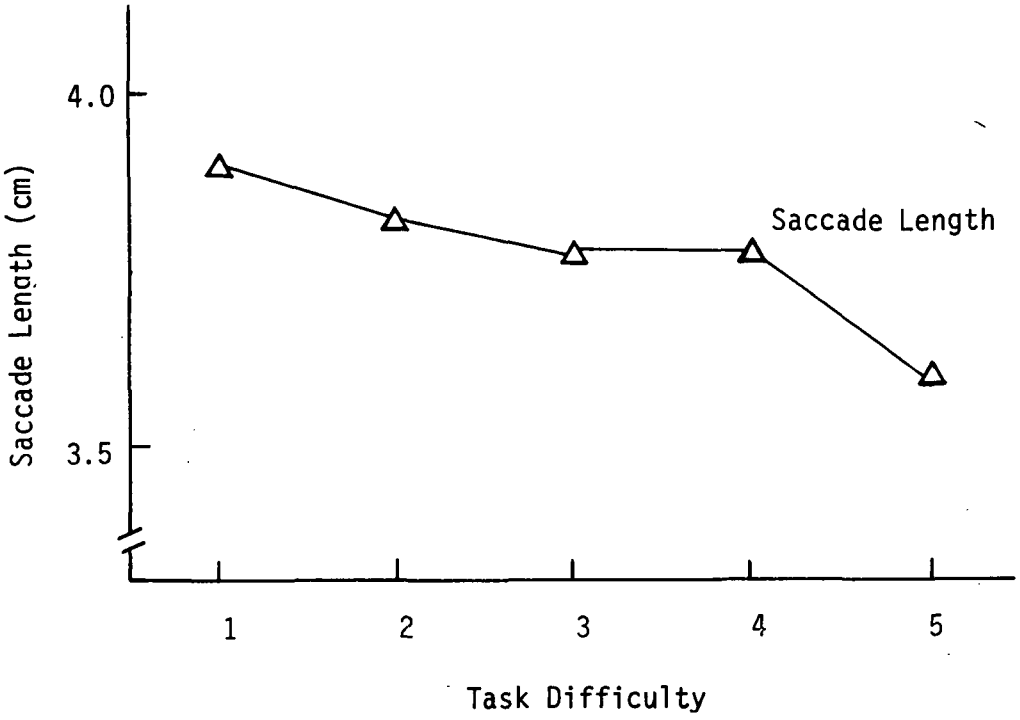

Figure 8. Average Change in Saccade Length as a Function of Changes in Task Difficulty

Table 11. Average Saccade Length by Subject, Event, and Level of Task Difficulty

	Level 1			Level 2			Level 3			Level 4			Level 5		
	Event			Event			Event			Event			Event		
Subject	1	3	5	1	3	5	1	3	5	1	3	5	1	3	5
1	----	5.77	3.40	----	6.20	3.56	----	6.12	4.09	----	6.17	4.04	----	5.97	3.61
2	4.22	3.15	2.92	4.67	2.87	2.62	4.32	3.33	2.51	4.52	2.92	3.96	3.45	2.36	3.38
3	4.93	2.74	1.88	4.09	2.31	1.24	3.56	2.31	1.47	4.52	2.11	1.42	3.53	2.03	1.63
4	3.96	3.86	2.74	4.22	3.56	2.82	3.96	3.18	3.25	3.63	3.20	3.43	3.45	2.87	2.74
5	3.66	3.45	2.01	3.78	3.99	2.18	4.04	3.30	2.08	3.25	3.56	1.93	3.76	3.73	2.18
6	6.60	4.72	4.27	6.43	4.45	3.66	5.49	4.47	3.68	6.63	4.72	4.29	5.51	4.47	3.76
7	5.21	4.72	4.45	4.93	5.08	3.48	5.69	4.75	4.27	5.66	4.50	3.02	5.36	4.37	3.68
8	4.50	3.86	3.96	4.32	4.11	4.95	4.85	3.89	3.61	4.47	3.78	5.03	3.53	3.61	5.08
Average	4.72	4.04	3.20	4.62	4.06	3.07	4.55	3.91	3.12	4.67	3.86	3.07	4.09	3.68	3.25

between saccade length and certain measures related to the ADI was investigated. Data for Subject 3 averaged only over replications of each condition is presented in Table 12. This particular subject was chosen because he demonstrated large decreases in saccade length across events and levels as compared to the other subjects.

In the first row of Table 12, decreases from Event 1 to Event 5 averaged as much as three centimeters. The question was: is this decrease due to more time spent on one instrument (the ADI) or to more transitions within the ADI, or to less scanning of peripheral instruments?

Note in Table 12 that ADI dwell time shows only a slight increase, the percentage of fixations a slightly greater increase, but the percentage of fixation transitions within the ADI (as opposed to cross checking other instruments) shows a marked increase across events. In addition, the percentage of within-ADI transitions for Event data increases across levels more than do the other measures.

The last row in Table 12 reflects the percentage of fixation transitions between the ADI and the instrument indicated. In each case, the instrument noted is the one most often fixated immediately before or after the ADI, typically the airpseed indicator. Adding the numbers in the last two rows together within a column yields totals very close to 100 percent in all cases for Event 5 data across the different difficulty levels. The issue of whether this is "appropriate" behavior in terms of relative amounts of information available in the various instruments or whether it demonstrates some evidence of the "locking on" phenomenon remains a question.

Table 12. Relationship between Saccade Length and Instrument Scanning Behavior for Selected Instruments. Data for Subject 3.

	Level 1			Level 2			Level 3			Level 4			Level 5		
	Event			Event			Event			Event			Event		
	1	3	5	1	3	5	1	3	5	1	3	5	1	3	5
Saccade Length (cm)	4.93	2.74	1.88	4.09	2.31	1.24	3.56	2.31	1.47	4.52	2.11	1.42	3.53	2.03	1.63
Percent ADI Dwell Time	81.2	90.8	96.8	86.4	94.1	98.9	86.5	94.6	98.4	85.0	95.5	97.3	92.3	96.0	98.9
Percent Fixations on ADI	73.5	83.5	90.9	79.1	87.7	96.4	80.2	88.4	39.3	79.8	90.9	93.9	86.6	89.6	97.7
Percent Transitions Within ADI	58.6	73.9	83.9	66.5	80.0	93.7	67.8	80.9	95.1	65.3	84.9	91.9	75.8	82.2	94.1
Percent Transitions Between ADI and:	9.2	4.1	7.0	6.1	9.6	3.6	11.4	6.5	2.8	8.2	7.3	3.6	7.7	6.0	2.3
	VSI	ASP	ASP	VSI	ASP	ASP	VSI	ASP	ASP	VSI	ASP	ASP	ASP	ASP	ASP

Because of the consistency found in Table 12 for within ADI transitions for Subject 3, similar data for all eight subjects were examined. The percentage of changes in fixation which began and ended on the ADI were included. These data were then averaged by level of difficulty and by flight segment (Event). Similar data were obtained for all the remaining instruments. Together, these numbers represent the sum of the diagonal of the fixation transition matrix. Both ADI transitions and all other within-instruments transitions are plotted in Figure 9 by level of difficulty and by event. As can be seen in Figure 9a, the percentage for both data sets rises slightly and fairly consistently as the level of task difficulty increases. From Level 1 to Level 5, the range is about five percent. In Figure 9b, a larger increase (about ten percent) is obtained across flight segments. While the changes are not as large as those reported in Table 12 for a single subject, they are reasonably consistent. Thus, the data suggest that the probability that the subject will remain on a given instrument increases as task difficulty increases.

FIXATION DURATION

If either the erratic scan pattern or locking-on behavior discussed above were to occur at higher workload levels, it would also likely result in noticeable changes in average fixation duration. Average fixation durations pooled across subjects as a function of task difficulty are shown in Figure 10 and by level and event for individual subjects in Table 13. Across levels, fixation duration shows a rather unsystematic trend. Within levels, the consistent trend is toward longer fixations as the pilot shifts from Straight and Level Flight (Event 1) to Flare and Touchdown (Event 5). This increase occurs in 75 percent of all comparisons; however, the differences are small, averaging one-tenth of a second or less. The increase may be due to the

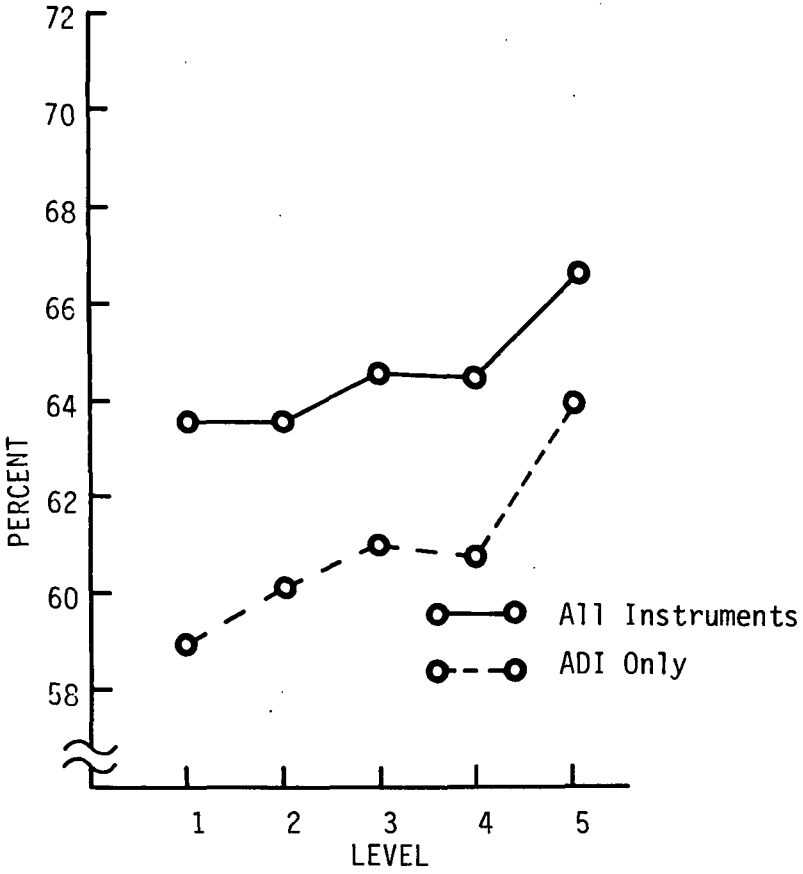

9a) Mean Across Events

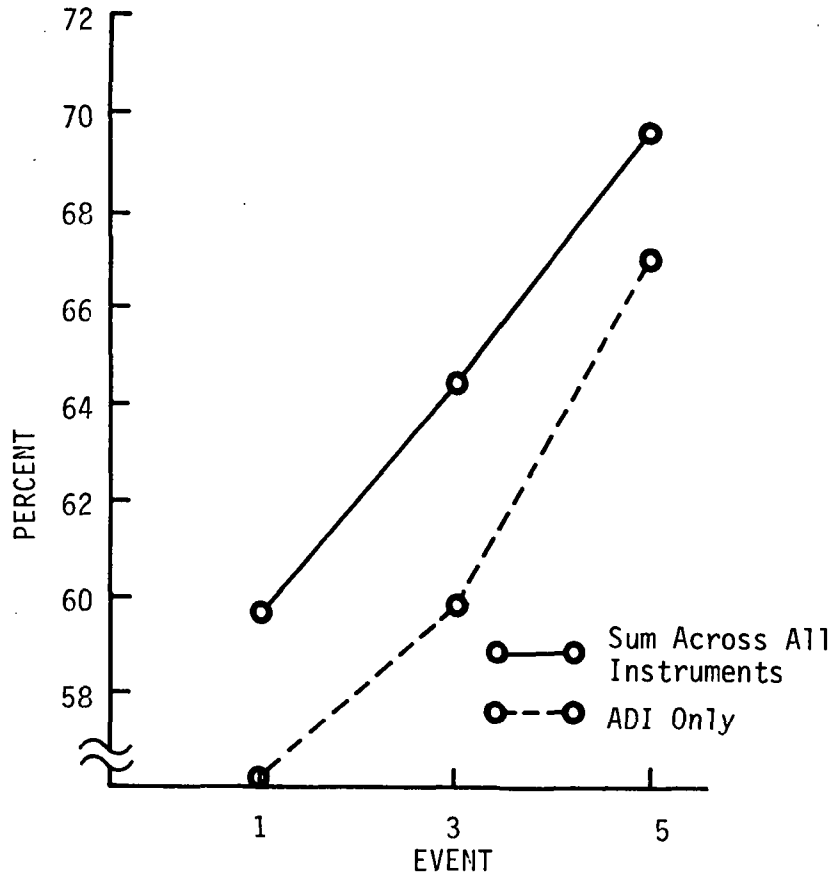

9b) Mean Across Levels

Figure 9a, b. Percentage of Transitions Within a Given Instrument (Sum of the Diagonal of the Transition Matrix) by Event and by Level of Difficulty

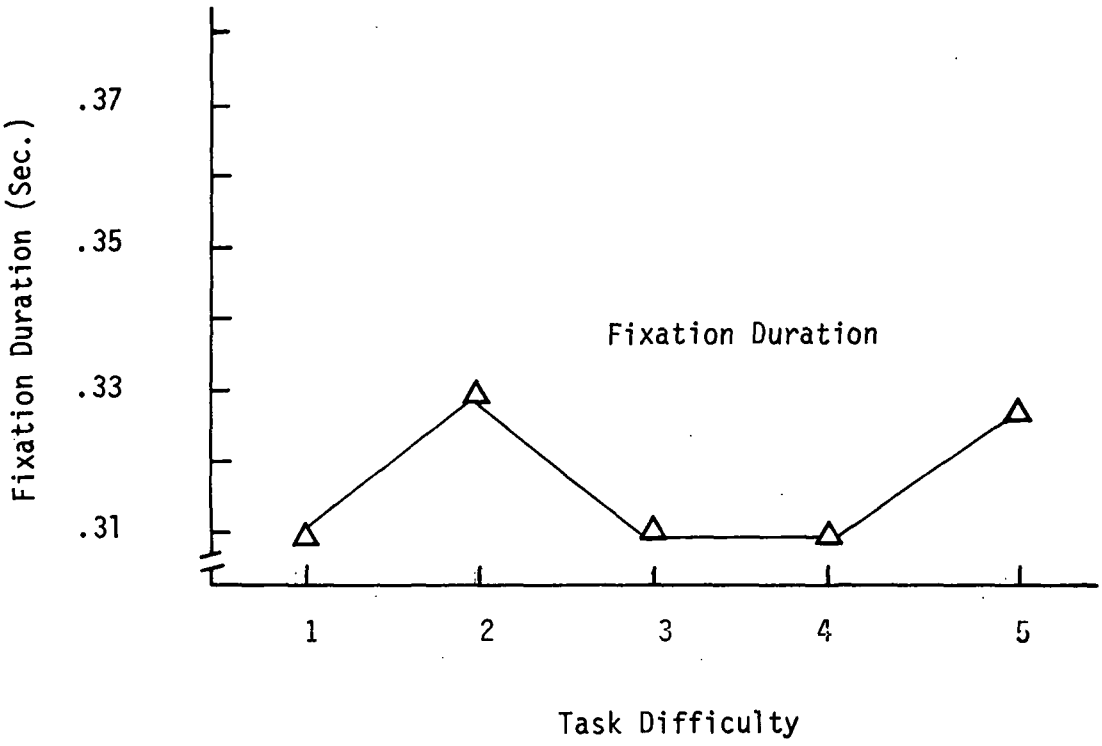

Figure 10. Average Change in Fixation Duration as a Function of Task Difficulty

Table 13. Average Fixation Duration by Subject for Each Event and Difficulty Level.

	Level 1			Level 2			Level 3			Level 4			Level 5		
	Event			Event			Event			Event			Event		
Subject	1	3	5	1	3	5	1	3	5	1	3	5	1	3	5
1	--	.28	.23	--	.29	.27	--	.27	.30	--	.25	.30	--	.29	.30
2	.24	.27	.26	.24	.28	.27	.26	.29	.33	.24	.28	.24	.28	.29	.30
3	.29	.41	.56	.34	.44	.65	.32	.47	.57	.30	.41	.47	.30	.47	.61
4	.28	.33	.42	.28	.35	.46	.29	.37	.39	.29	.37	.35	.30	.39	.44
5	.44	.33	.41	.38	.36	.58	.30	.30	.42	.30	.34	.45	.47	.32	.47
6	.26	.24	.32	.26	.25	.38	.26	.24	.33	.23	.24	.33	.25	.28	.37
7	.28	.27	.29	.29	.24	.28	.26	.25	.30	.26	.28	.40	.23	.29	.36
8	.22	.22	.22	.23	.23	.22	.22	.24	.25	.25	.27	.23	.20	.21	.24
Average	.29	.29	.34	.29	.31	.39	.27	.30	.36	.27	.31	.35	.29	.32	.39

fact that the pilot is seeking more rate information as he approaches touchdown. It is interesting to note, however, that both saccade length and fixation duration data exhibit trends which are suggestive of the locking-on hypothesis. The fact that the changes are more marked across events than across levels implies that either the change in workload was greater within a run as touchdown was approached, or, as was suggested above, it merely reflects a change in the type of information the pilot is using as he approaches touchdown, that is, more rate information.

BLINK RATE

Blink rate data, unlike the other measures, were not obtained from the digitized flight data. Video tapes of the pilot's eye were obtained for each of the 200 runs. When the pilot blinked, it was clearly indicated on the video tape. For all runs, a count of the total number of blinks was made. Data for each subject and level of difficulty were obtained. These are shown in Table 14 and Figure 11 respectively. As can be seen, there is a tendency for blink rate to decrease as the level of task difficulty increases. The absolute value of this difference is quite small, however.

PUPIL DIAMETER

Results of the general Stepwise Linear Regression Analysis presented earlier in this section (Table 8) indicated that pupil diameter was the one and only variable of all those studied which demonstrated a strong predictive relationship with pilot workload, that is, the Cooper-Harper ratings. There is evidence in the literature which supports this relationship. Bradshaw, 1968, (Reference 2) found that pupil diameter increased both as a function

Table 14. Average Number of Blinks Per Trial by Subject and Level of Task Difficulty.

Subject	1	2	3	4	5
1	10.28	10.92	11.36	9.70	10.08
2	3.36	3.68	3.56	2.24	2.40
3	10.80	9.60	7.00	8.00	7.80
4	1.76	2.36	2.24	1.52	1.44
5	2.08	2.68	2.56	2.28	3.20
6	11.04	12.28	11.88	10.56	14.08
7	9.16	10.08	9.40	9.24	7.88
8	5.52	4.72	5.12	4.16	3.64
Average	6.66	7.04	6.64	5.96	6.32

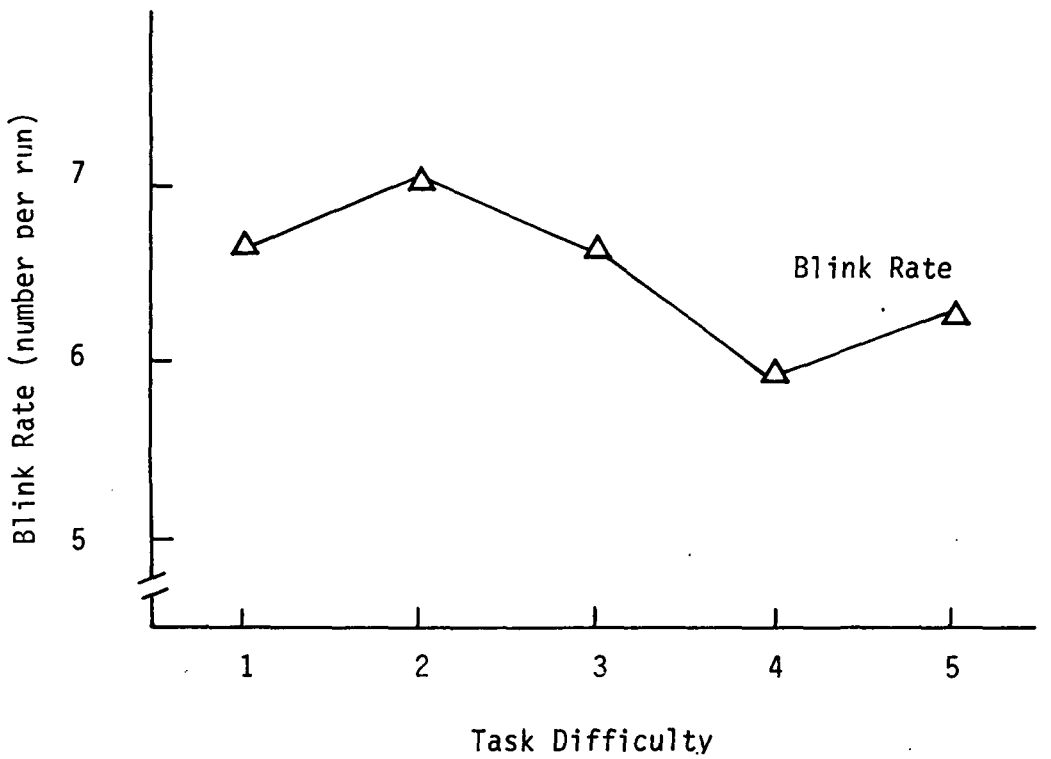

Figure 11. Average Number of Blinks Per Run as a Function of Task Difficulty.

of rate of stimulus presentation and task complexity in a task involving the continuous processing of alphanumeric information. Simpson and Hale, 1969, (Reference 8) found similar effects in a decision-making task. Payne, et. al., 1965, (Reference 6) and Hess and Polt, 1967, (Reference 3) found that pupil diameter increased as the difficulty of a mental arithmetic problem increased. These studies are examples of previous research concerned with the relationship between pupil diameter and task difficulty. The positive results obtained suggested that this variable might be of value in the present analysis. The results of the general stepwise linear regression analysis reported above (See Table 8) supported this hypothesis.

In Table 15, average pupil diameter is presented by subject as a function of flight segment (Event) and difficulty level. Average data across subjects are presented in Figure 12. In spite of a rather large variability between subjects, trends can be seen within subjects. Pupil diameter tends to increase across events within a level although there is very little change across levels. While the magnitude of these changes averages only about two to four percent, the changes are rather consistent in direction. In fact, 72 percent of all comparisons between Event 1 versus Event 3 and Event 3 versus Event 5 showed an increase.

Earlier research (Reference 3, Hess and Polt, 1964) bad reported changes in pupil diameter as large as 30 percent over a baseline condition. The task used in this study (mental arithmetic) lasted only a few seconds, as compared with the present data which were averaged over as much as five minutes. It was possible, therefore, that the small changes observed were due to averaging over prolonged time intervals. It was also possible that pupil diameter changes would be most marked in reaction to increases or decreases in

Table 15. Average Pupil Diameter (millimeters) by Subject, Event, and Level of Task Difficulty

Subject	Level 1			Level 2			Level 3			Level 4			Level 5		
	Event			Event			Event			Event			Event		
	1	3	5	1	3	5	1	3	5	1	3	5	1	3	5
1	--	7.80	8.08	--	7.94	8.19	--	7.87	8.33	--	7.80	8.01	--	7.91	8.15
2	8.58	8.75	8.68	8.61	8.79	8.79	8.61	8.75	8.75	8.47	8.65	8.19	8.61	8.83	8.68
3	6.28	6.60	6.85	6.35	6.46	6.60	6.25	6.50	6.53	6.35	6.50	6.71	6.50	6.64	6.74
4	6.74	6.53	6.42	6.71	6.42	6.35	6.67	6.50	6.60	6.85	6.67	6.57	6.85	6.71	6.60
5	5.15	4.91	5.44	5.01	5.12	5.54	5.12	4.91	5.40	5.12	5.19	5.40	5.15	5.22	5.75
6	6.57	7.06	7.34	7.10	7.17	7.48	6.95	7.06	7.31	6.85	7.10	7.27	6.74	7.13	7.41
7	7.27	7.10	7.17	7.10	7.02	7.10	7.20	7.06	7.02	7.10	7.13	7.31	6.92	7.06	7.13
8	6.14	6.28	6.57	6.32	6.32	6.35	6.46	6.46	6.60	6.21	6.25	6.60	6.32	6.39	6.53
Average	6.71	6.88	7.10	6.74	6.92	7.06	6.74	6.88	7.02	6.71	6.92	7.02	6.74	6.99	7.13

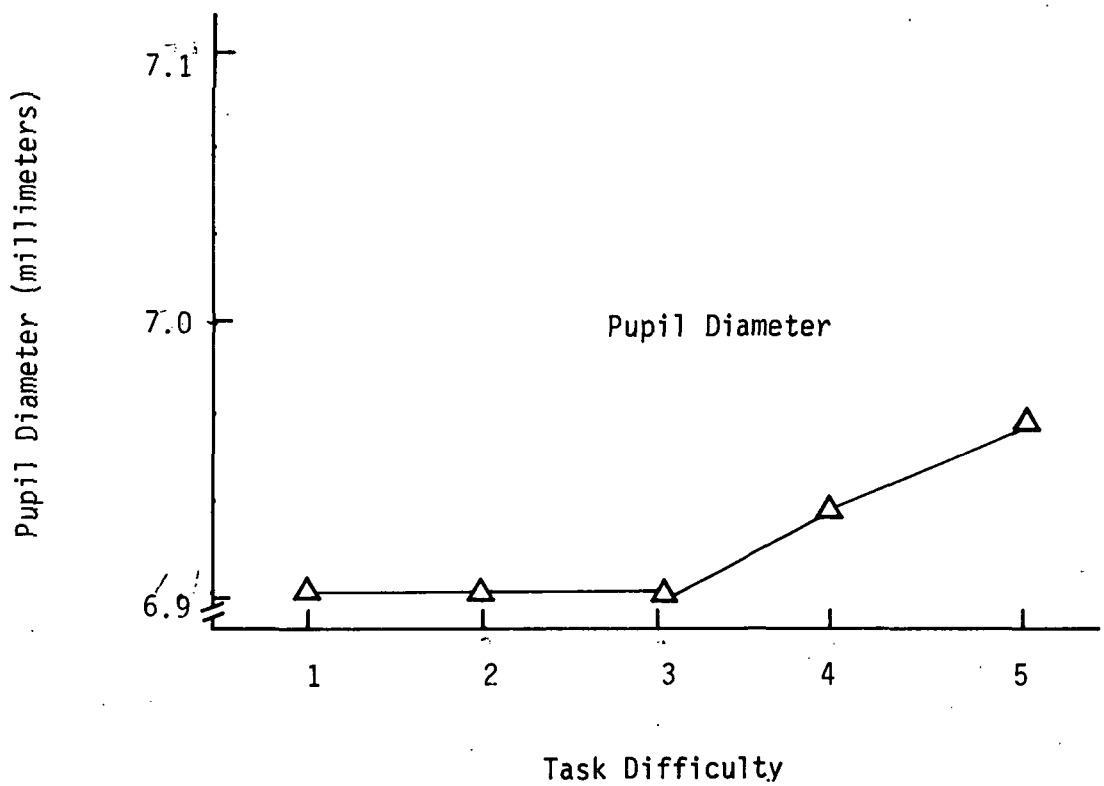

Figure 12. Average Change in Pupil Diameter as a Function of Task Difficulty

error on one of more of the state variables. To investigate this, individual run data were examined by preparing short time history plots for each of the 200 runs. In each plot, state variable error and pupil diameter were plotted as a function of time into run. An example of two such plots, one for Level 1 and one for Level 5, are presented in Figure 13 which shows the relationship between pupil diameter changes and changes in error for command airspeed, localizer, and glideslope. Each of these plots was examined by eye to determine if a more comprehensive analysis was warranted.

While marked fluctuations in pupil diameter were observed over time, there appeared to be no consistent relationship between state variable error and pupil diameter. This conclusion was supported by a similar lack of correlation between instrument dwell time and pupil diameter at the more general level of analysis reported earlier in Table 7, which was based on data averaged over entire runs.

Calculations of pupil diameter are slightly affected by eye rotation relative to the mirror system in the oculometer. To determine if this change was larger than expected and a source of confounding, pupil diameter was calculated individually for each instrument. This was done by calculating average pupil diameter over all fixations on a given instrument. Differences were observed among instruments but again the differences were small (less than one millimeter) and not consistent in magnitude or direction.

Even though pupil diameter averages did not vary widely, additional analyses were performed using ADI-related pupil diameter data. The ADI was chosen because a great majority of all fixations were on that instrument. In Figure 14, pupil diameter is plotted for two different subjects, one run at Level 1

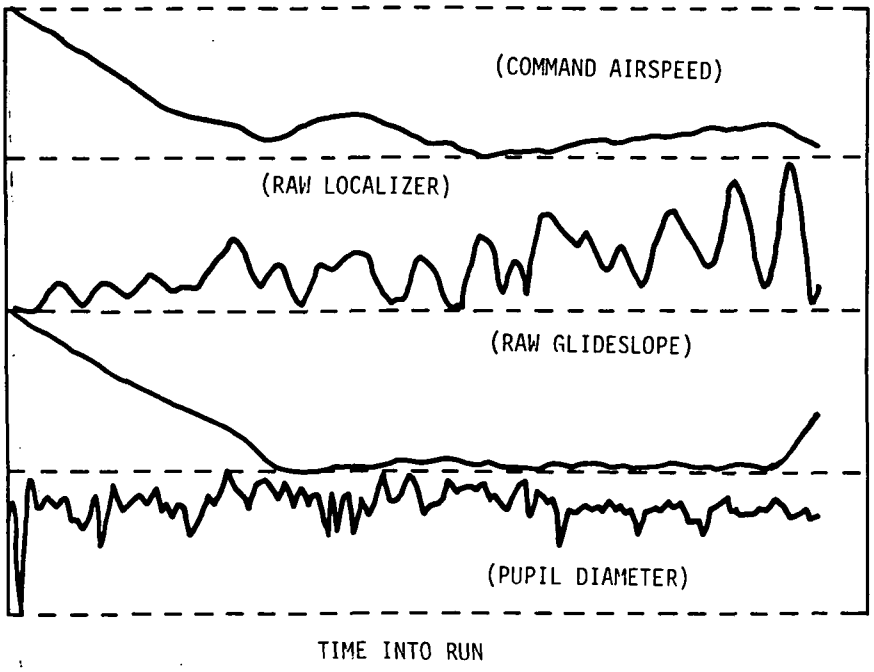

A. Data for Level 1 (Low Workload)

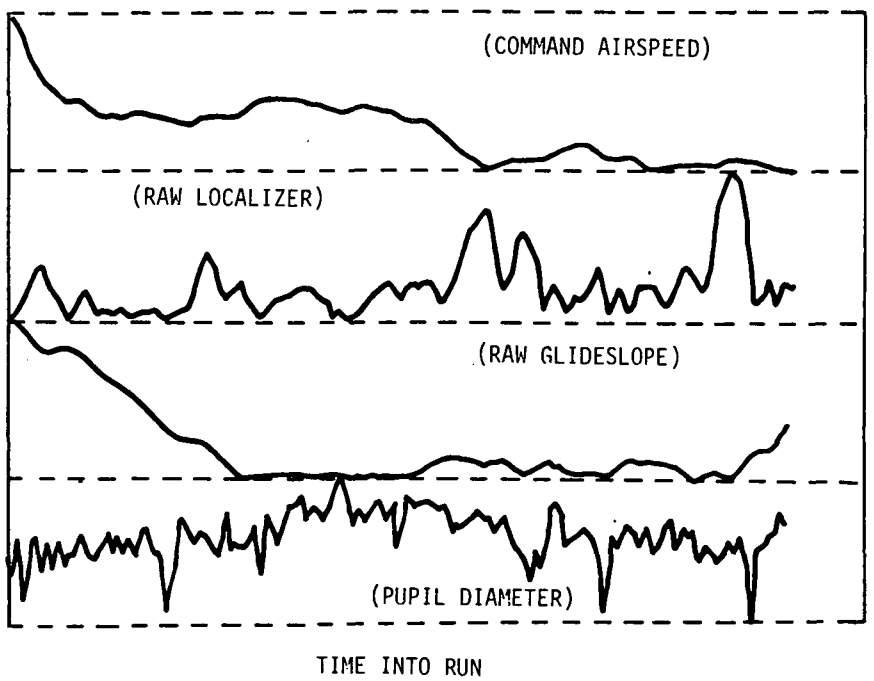

B. Data for Level 5 (High Workload)

Figure 13. Short-time History Plot of Errors for Three State Variables and Pupil Diameter. Data for Subject 2.

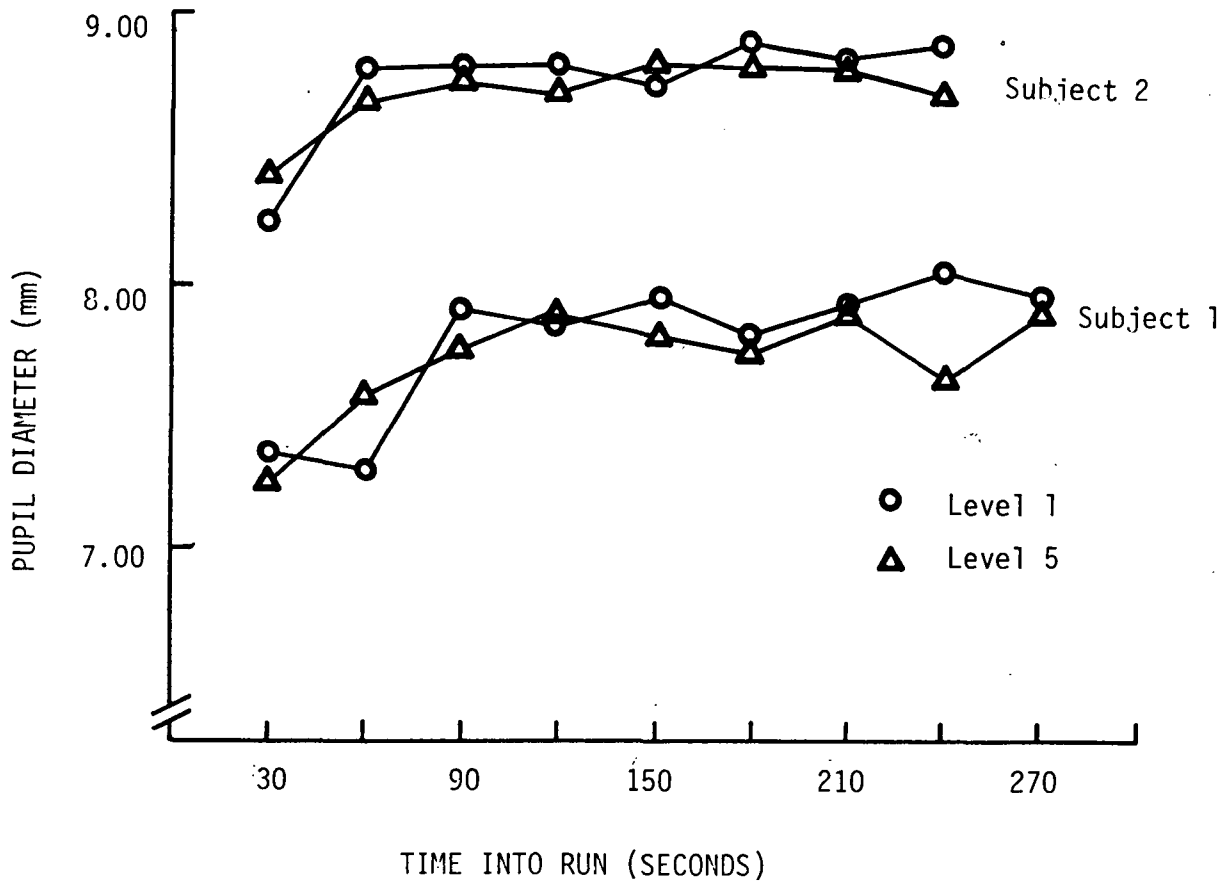

Figure 14. Pupil Diameter Data for Individual Runs by Individual Subjects at Two Levels of Task Difficulty. Data are Calculated only during Fixations on the ADI.

and one at Level 5 for each. The data were calculated from samples of ADI fixations only and are averaged over 30-second intervals. The plots show a trend toward larger pupil diameter for the more difficult Level 5 runs and a slight trend toward larger pupil diameter as time into run increases. However, as was found with the average data reported earlier, the changes are extremely small.

As a final attempt at understanding the nature of the pupil diameter variable, a series of Stepwise Linear Regression Analyses were computed. The dependent variables were pupil diameter measures calculated individually for each of the ten instruments. Data were averaged over 30-second time intervals for each run. As was done with the dwell time data, regression analyses were performed for individual subjects and for all subjects over various time segments. The resulting R^2 values were extremely low for all tests, typically around 0.25 and none as high as 0.40. Thus, when segmented by instrument and averaged over short time intervals, pupil diameter accounted for less than 40 percent of the variance in the Cooper-Harper ratings.

PUPIL DIAMETER RE-EXAMINED

The closer examination of pupil diameter was initially undertaken to clarify the nature of its relationship to pilot workload. In light of that objective, the above results were quite unexpected. How can the conflicting findings be reconciled? Why was the strong relationship with workload lost when the pupil diameter data were partitioned by instrument?

The most reasonable explanation that can be offered at this point is that two different variables were being examined in the two different sets of regression analyses. In the partitioned set performed last, it is probable that a "true" measure of pupil diameter was being evaluated. It showed no strong relationship to workload.

The initial regression analysis which showed the strong relationship between pupil diameter and workload was most likely not a pure measure of pupil diameter. It is suggested that this general variable pooled across instruments and averaged over entire runs is a composite variable reflecting both actual pupil aperture and some measures related to relative time spent on the various instruments. For example, the image of the pupil as sensed by the oculometer becomes slightly eliptical as the eye rotates away from center. Thus dwells on peripheral instruments would produce distorted measures of pupil diameter. This fact combined with actual changes in pupil size might result in some systematic "workload" related trend.

If this argument is valid, and the variable is not in fact purely pupil diameter, it in no way diminishes its potential value. On the contrary, it should be noted that this more general measure indicates a relationship that neither dwell time data or instrument-specific pupil diameter alone demonstrated.

PILOT PARAMETER ESTIMATION

In this sub-section, results of an independent analytical effort performed under this contract are discussed. The oculometer data were used as the basis for selecting samples of data from within a run. Interest was focused on the ADI since it provides so much flight-related data on one instrument.

In part, the analysis concentrates on determing what information the pilot is using as he dwells for prolonged periods on the composite flight director.

Maximum Likelihood Estimation (MLE) software was used to estimate pilot parameters with established model structures. These estimates were referenced to the eye location, as supplied by the oculometer, to determine the characteristic pilot behavior for various tasks associated with landing approach. Some theoretical considerations of MLE are presented in Appendix C.

A brief history of pilot modeling follows.

"Crossover" Pilot Model

Pilot modeling using parameter fits to pre-defined dynamic structures has been developed over a number of years. McRuer and Krendel, 1957 (Reference 4) developed the initial model based upon cascaded "classical" dynamic elements defined in the frequency domain. This model can be described as follows for single-axis compensatory tasks:

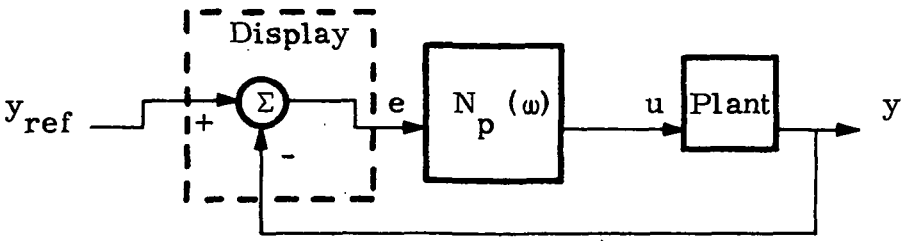

(3)

where

N_p (ω) = the pilot describing function

y_{ref} = the commanded track state

y = the actual track state

e = the displayed track error

The describing function, $N_p(\omega)$, is

$$N_p(\omega) = K_p \frac{(T_{Ld}S+1)}{(T_{Lg}S+1)} e^{-\tau s} \qquad (4)$$

τ = computational delay (fixed and known)

T_{Lg} = neuromuscular lag

T_{Ld} = pilot lead compensation

K_p = pilot gain

The parameters provide the key clues to pilot workload and stress. The computational delay, τ, is variable in human beings but is fairly consistent for trained pilots. $\tau = 0.2$ second is sufficient for most purposes.

The neuromuscular lag, T_{Lg}, varies with task difficulty: a large value indicates an easy task, that is, pilots can be a little lazy, and a small value represents more difficult tasks.

The lead time constant, T_{Ld}, represents the pilot's attempt to differentiate a displayed quantity. This occurs for plants that exhibit larger than first order roll off characteristics at the plant/pilot crossover region (i.e., more difficult tasks).

The pilot will adjust his gain, K_p, to obtain a -1 frequency response slope at the crossover point, that is, he likes to have the pilot plant system behave as an integrator at the dominant control task frequency.

Optimal Pilot Model

The use of optimal control theory (Reference 1, Baron, et. al., 1970) is a method of estimating pilot dynamic behavior using time measurements as opposed to the frequency domain approach. Based upon the argument that the pilot attempts to optimize his performance for a given task, the use of the optimal control approach extends the classical model in a number of areas:

- explicit structure to multi input/multi-output systems
- more explicit treatment of scanning behavior, task interference, and operator workload
- state-space formulation to allow application of powerful numerical algorithms to obtain desired parameters efficiently
- theoretical noise treatment embedded into the formulation

Optimal "Estimated" Pilot Model

The use of parameter estimation techniques such as maximum likelihood (Reference 7, Phatak , 1975) allows further refinement to the optimal model by reducing the number of arbitrary parameters to be chosen, quadratic performance index weights, for example.

There are some conflicting arguments between these last two techniques (Reference 7, Phatak, 1975) but they are mostly based on heuristic assumptions made by each model. Results for both are good.

Parameter Estimation with Scanning Information

The data created using the oculometer provide a unique set of information for looking at pilot dynamic behavior. Previous studies (For example, Reference 7, Phatak, 1975) did not have the luxury of knowing exactly where the pilot was looking on the instrument panel.

The earlier models discussed use an additive noise term to account for scanning. Sometimes called a pilot remnant, the effect is to degrade primary axis tasks with assumed scanning behavior.

For the present study, the certain knowledge of pilot attention allows removal of remnant over a given period of time.

Pilot Model Structure

As described in Appendix C, a state space form of the model is used in the identification. Figure 15 shows the model employed in the current analysis. This structure was used because it has the potential for reconstructing Equation (4) for each input/output pair. In continuous state space, this model would be

$$\dot{x} = Fx + G_1 u + G_2 \eta \tag{5}$$

$$y = Hx + Du + \xi \tag{6}$$

where:

$$F \triangleq -\left[\frac{1}{T_{Lg}}\right] \qquad \text{(scalar)}$$

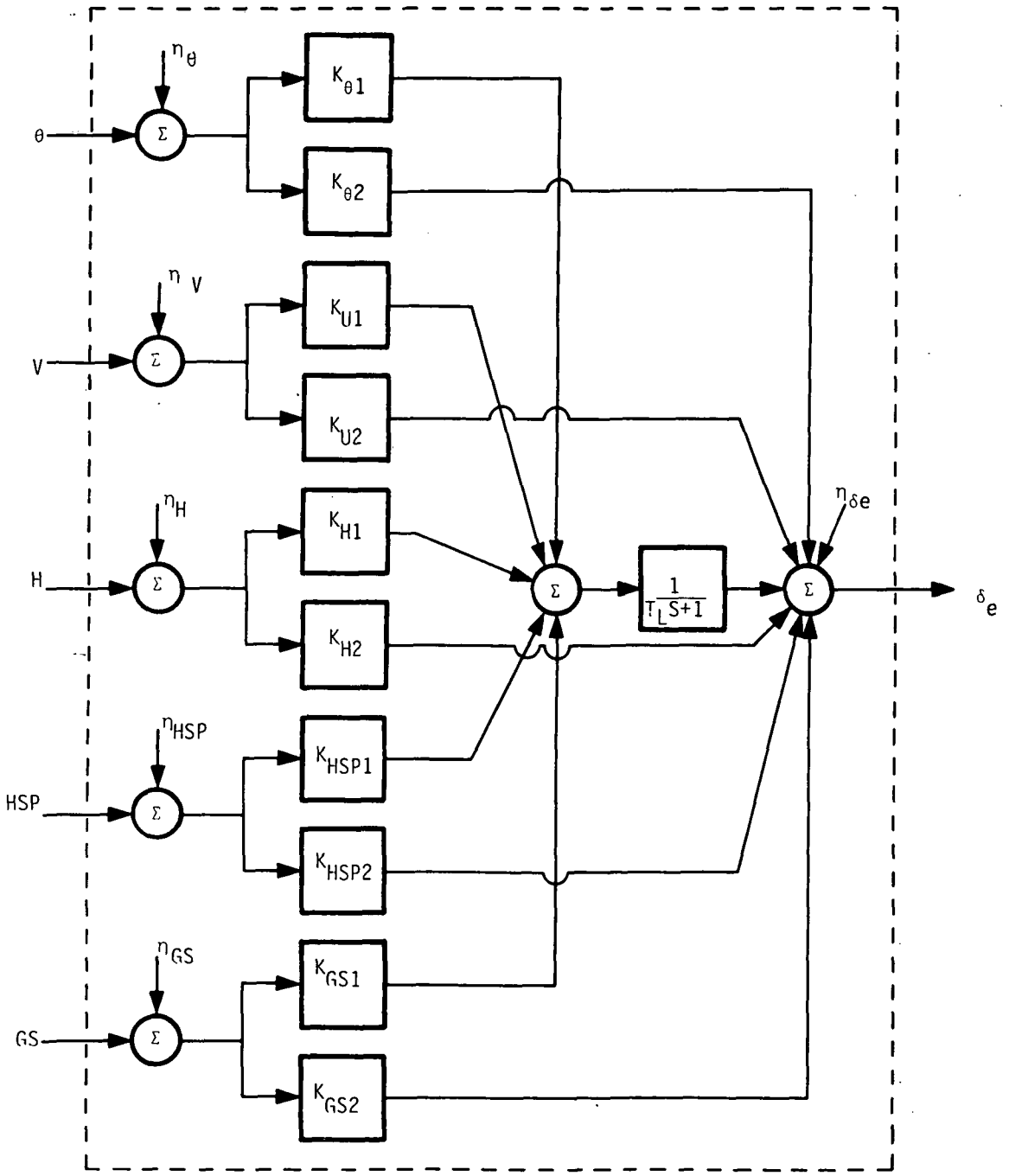

Figure 15. Pilot Model Structure

$$G_1 \triangleq \frac{1}{T_{Lg}} \left[K_{\theta_1}, K_{V_1}, K_{H_1}, K_{HSP_1}, K_{gs_1} \right]$$

$$G_2 \triangleq [I] \quad \text{(identity matrix)}$$

$$H \triangleq [1] \quad \text{(scalar)}$$

$$D \triangleq \left[K_{\theta_2}, K_{V_2}, K_{H_2}, K_{HSP_2}, K_{GS_2} \right]$$

$$X^T \triangleq (\theta, V, H, HSP, GS)$$

$$y \triangleq \delta e$$

$\eta \triangleq$ observation noise $\sim N^*(0, \sigma_{ON})$ white

$\xi \triangleq$ motor noise $\sim N(0, \sigma_m)$ white

The MLE software descretizes this model for calculations and converts final results back into continuous form.

RESULTS OF MAXIMUM LIKELIHOOD ANALYSIS

Results were generated for one pilot flying through the sequence of five events from probelm entry to touchdown. The sequences were chosen from oculometer results which indicated sole concentration on the ADI.

The initial observation is that in all cases the time constant parameter approached large values. This forced the lag term into an integrator. The gain values, therefore, reflected relative amounts of proportional plus integral control, used by the pilot for a given input variable.

---

*N(m, σ) = normal distribution with mean 'm' and variance 'σ^2'.

The most revealing results consisted of examing the weighted residual portion of the likelihood function (Appendix C).

Let:

$$R = \Sigma_{i=1}^{n} \; v_i \beta v_i^{-1} \tag{7}$$

where β_i = apriori residual covariance matrix

$v_i = \delta e_a - \delta e_p$

δe_a = Actual Fore-aft Stick Position

δe_p = Predicted Stick Position of the Identification (at the ith time epoch)

This response gives a good indication of the ability of the identification to reconstruct the actual stick position.

To find the dominant variables in the system, gains were sequentially set to zero and predicted stick position, δe_p, was recalculated without the benefit of the entry of a given variable into the system. Critical inputs would naturally have a larger impact upon the residual response, R; that is, the larger the deteriorization of the response implies, the more important gain value is to the reconstruction.

Table 16 displays the results of this sensitivity analysis. Specific conclusions are:

1. Results correlate well with the overall control task, i.e., the the dominant variables were the important ones for specific control tasks.

Table 16. Likelihood Function Parameter Sensitivity

$R = \Sigma_{i=1}^{n} \; B_k^{-1} \; \nu_i^2$

ELIMINATED PARAMETER	EVENT 1 (Level flight)		EVENT 3 (Descent)			EVENT 5 (Flare to touchdown)		
	ADI dwell 1	ADI dwell 2	ADI dwell 3	ADI dwell 4	ADI dwell 5	ADI dwell 6	ADI dwell 7	ADI dwell 8
None	2.098	3.46	57.72	42.79	7.73	1.78	16.9	.0785
T_L	424.3	107.3	$3.15X10^4$	$7.00X10^5$	$7.02X10^3$	$3.53X10^3$	805.3	$6.70X10^3$
K_{GS1}	not used	not used	$1.4X10^{7**}$	$7.69X10^{6**}$	$7.82X10^4$	13.0	$1.82X10^{7**}$	$1.56X10^{6*}$
K_{V1}	1008.9**	60.86	$7.14X10^4$	$7.40X10^3$	$6.61X10^3$	388.8	$1.35X10^4$	$4.28X10^3$
K_{H1}	157.0	10.77	$1.39X10^{7**}$	$2.16X10^{6**}$	$2.03X10^4$	890.1	$1.57X10^{7**}$	$1.24X10^{6**}$
K_{E1}*	2.15	3.46	$1.27X20^5$	$6.56X10^{6**}$	$7.88X10^2$	$2.81X10^3$	$1.97X10^4$	16.9
$K_{\Theta 1}$*	119.9	54.50	$1.78X10^4$	$4.90X10^5$	$3.06X10^5$	$1.06X10^{4**}$	$5.31X10^3$	4.26
K_{GS2}	not used	not used	$2.11X10^4$	$2.13X10^{6**}$	$3.74X10^{6**}$	$3.16X10^{5**}$	$2.85X10^4$	$8.79X10^{5**}$
K_{V2}	6.18	68.20	439.0	105.6	$1.68X10^2$	4.02	49.9	$107.0X10^2$
K_{H2}	353.7	52.38	$4.81X10^5$	$2.24X10^5$	$3.40X10^{6**}$	$2.06X10^{5**}$	$5.08X10^3$	$9.26X10^{5**}$
K_{E2}*	2.10	3.46	$4.63X10^5$	$1.47X10^5$	$1.35X10^4$	$2.68X10^{4**}$	$2.94X10^3$	518.2
$K_{\Theta 2}$*	8.38	115.6**	$1.44X10^5$	$7.25X10^3$	$5.27X10^3$	26.4	$5.79X10^3$	$2.49X10^4$
Time on	29.8	43.7	86.0	103.7	189.8	250.8	257.8	267.8
Dwell	3.1 sec	4.1 sec	7.5 sec	9.4 sec	3.8 sec	2.9 sec	5.2 sec	1.6 sec
Time off	32.9	47.8	93.5	113.1	193.6	253.7	263.0	269.4

* Indicates variable display on ADI

** Recognized as having a relative major influence

Variable definitions: T_L = Lag time Constant; GS = Row glide slope; ν = Velocity; H = Altitude; E = Horizontal Steering pointer

2. Higher impact from the horizontal steering pointer might have been expected; however, in general it does not greatly affect the identification relative to other variables.

3. Some shift of emphasis can be noticed from integral to proportional influences as the approach proceeds in time. This possibly indicates a shift in workload, that is, integral control implies a less difficult task.

Also shown in Figures 16 through 22 are comparison plots of actual stick position and generated stick position based upon identified parameters. The actual plots, shown on top of each figure, contain a 12 cycle/second nuisance which, although low-passed before analysis, still shows up. The reconstructed stick position, however, should not and does not reflect this as no provision in the model was made to account for this.

Some open questions:

1) Do the influential variables imply that the pilot actually picked up peripheral information (altitude and glideslope)?

2) Is the reason for their high impact related to the overall control task and not the display layout?

The second alternative seems more likely. The fact that the ADI dwell is predominant implies that attention is given to the horizontal steering pointer. The pilot can get the appropriate path control information from this variable. Hence, he is controlling altitude and glideslope from the pointer.

Figures 16 through 22, referenced on page 72, follow on the next 14 pages. The plots (actual versus generated) for each ADI Dwell appear on facing pages.

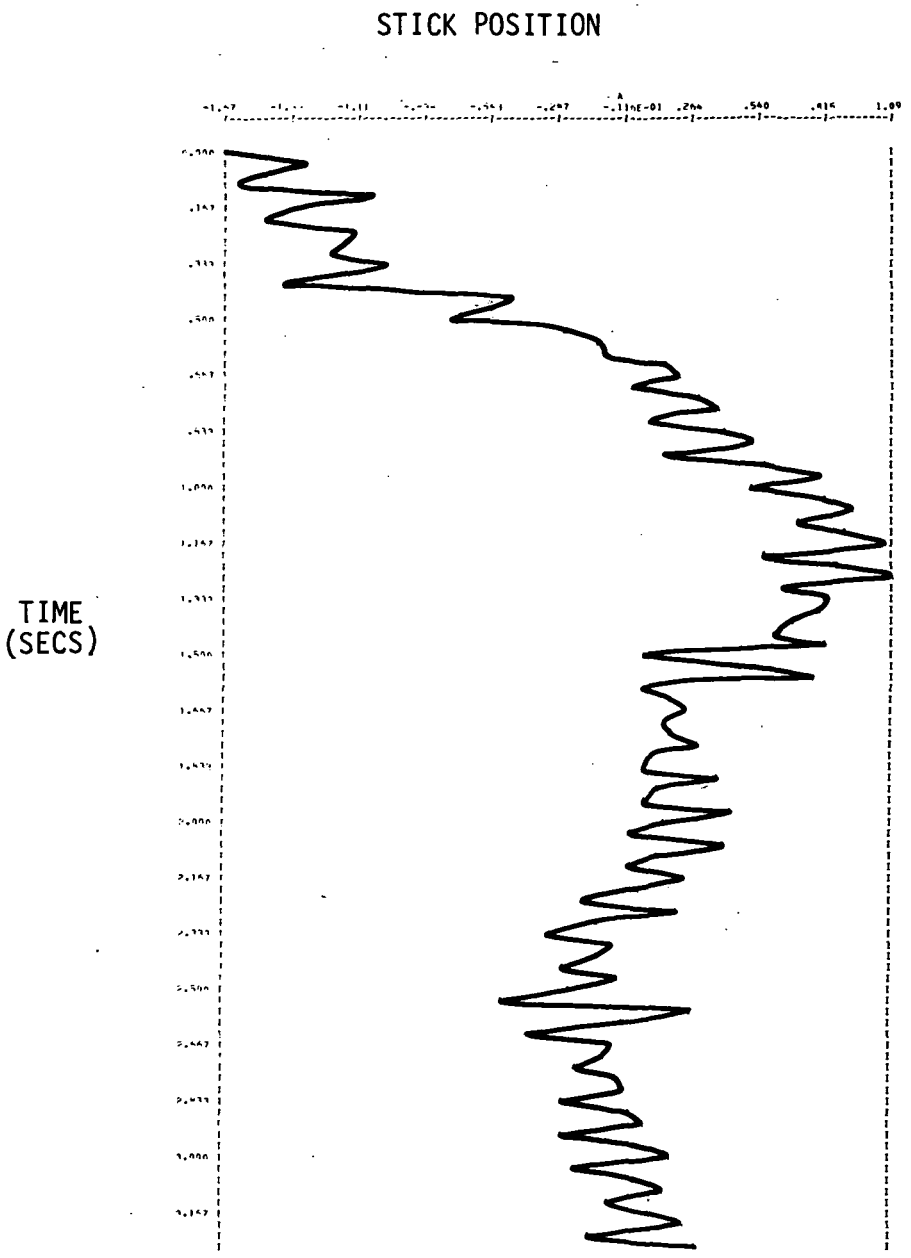

a) Actual Stick Position

Figure 16. ADI Dwell 1

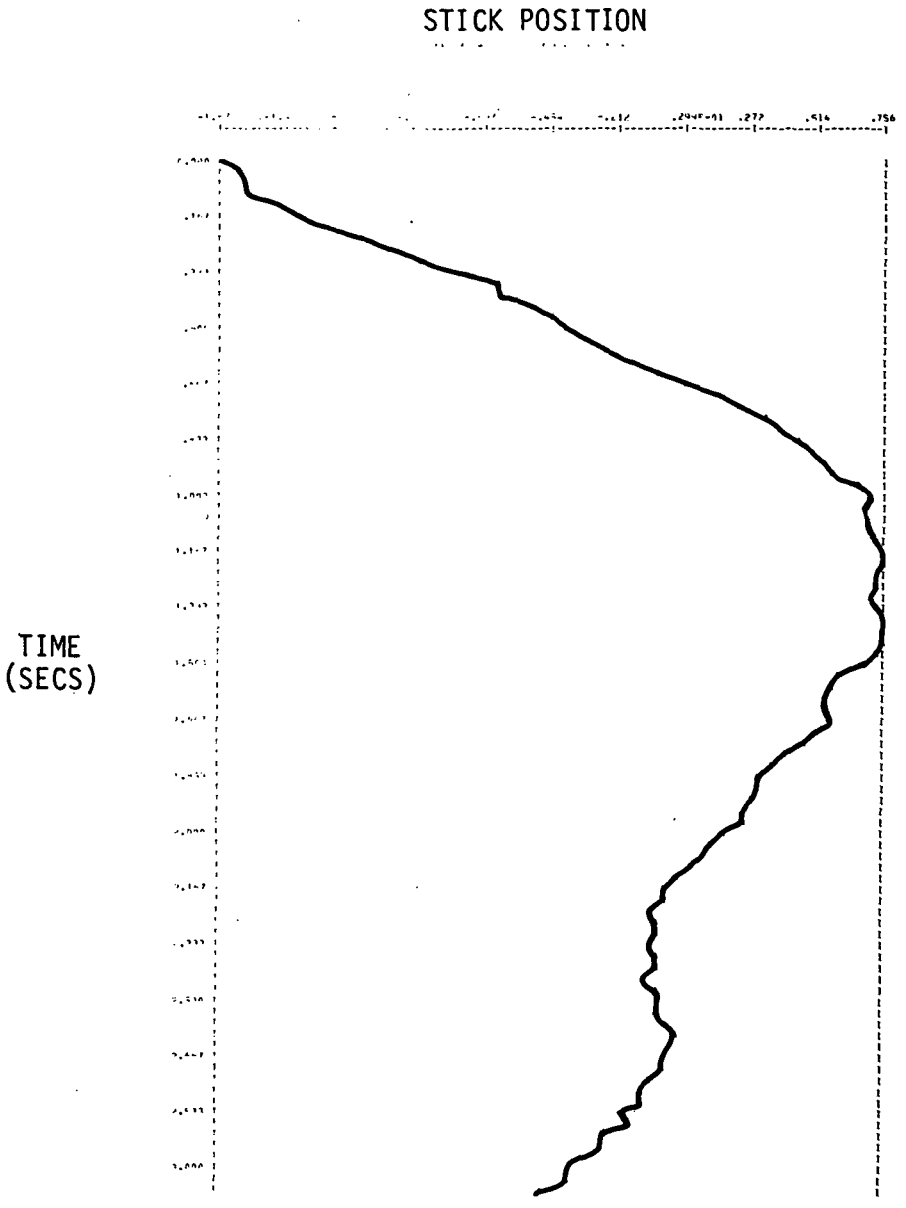

b) Generated Stick Position

Figure 16. ADI Dwell 1

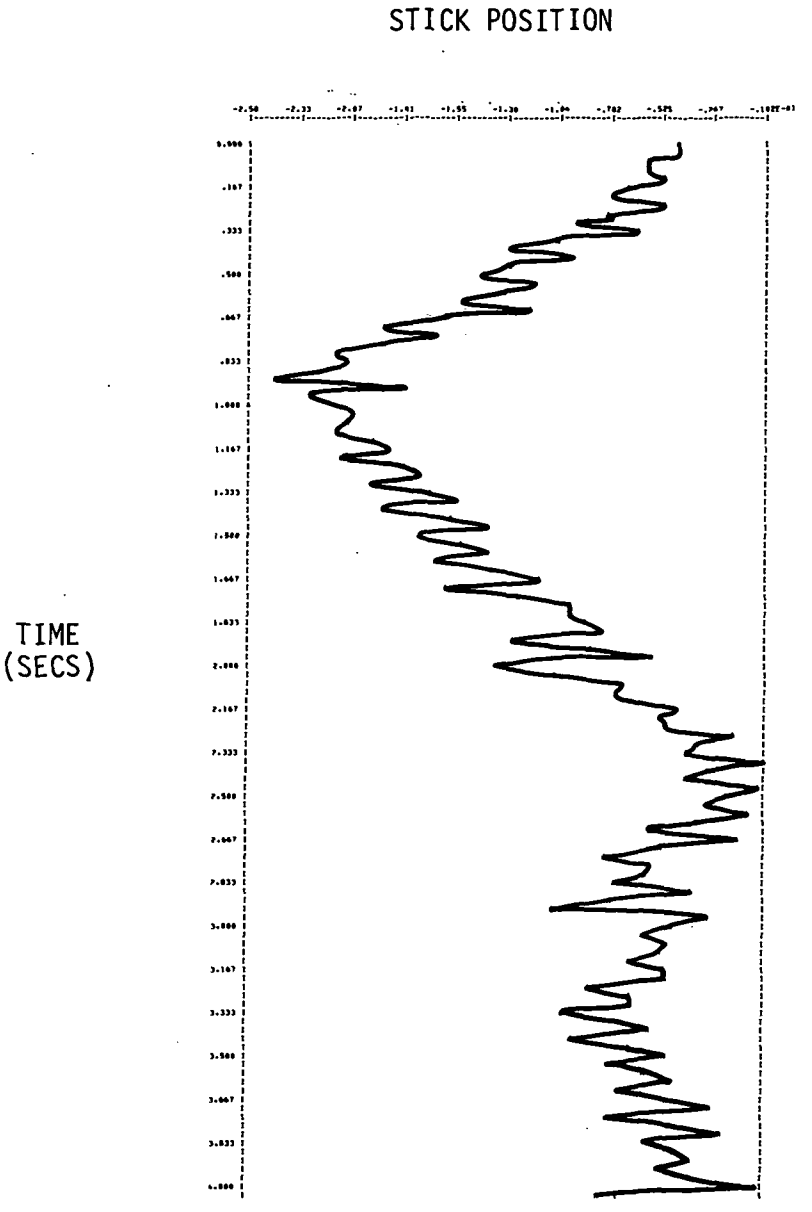

a) Actual Stick Position

Figure 17. ADI Dwell 2

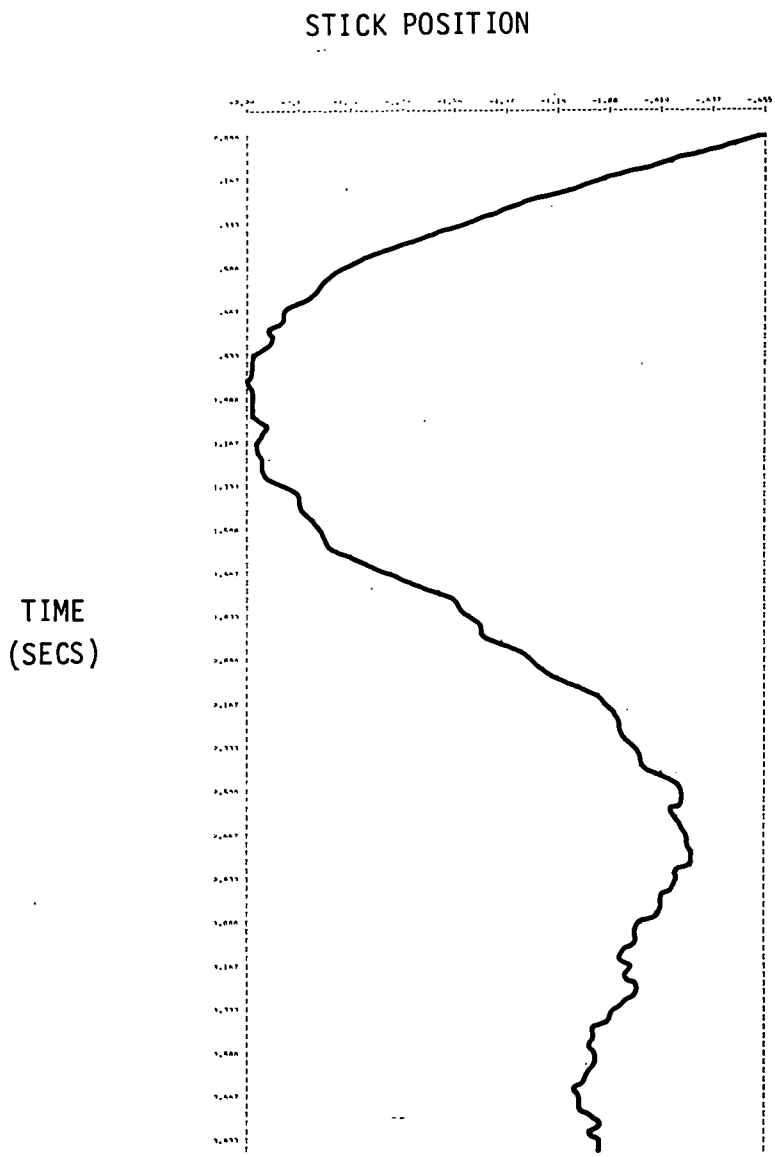

b) Generated Stick Position

Figure 17. ADI Dwell 2

STICK POSITION

TIME
(SECS)

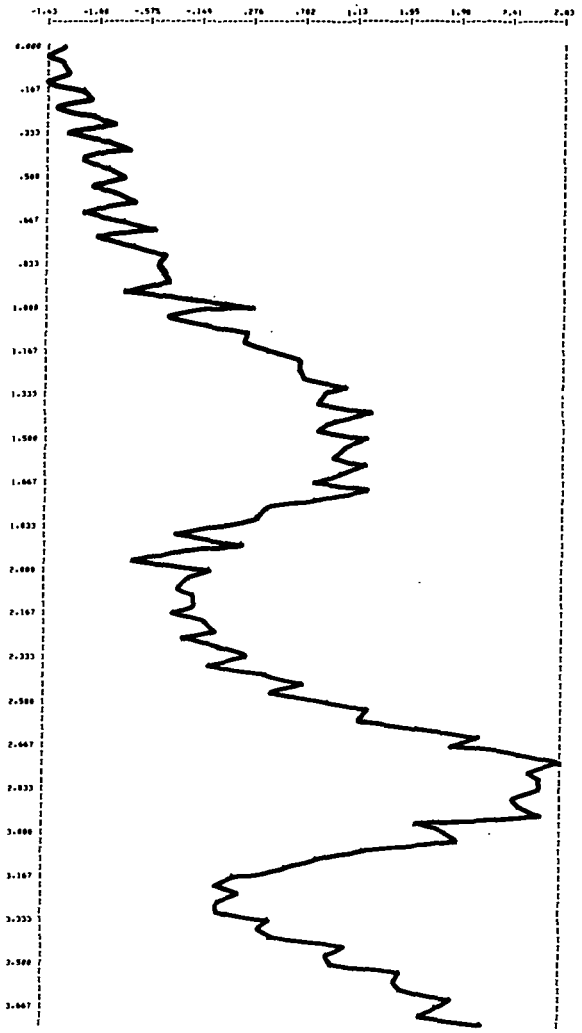

a) Actual Stick Position

Figure 18. ADI Dwell 3

STICK POSITION

TIME
(SECS)

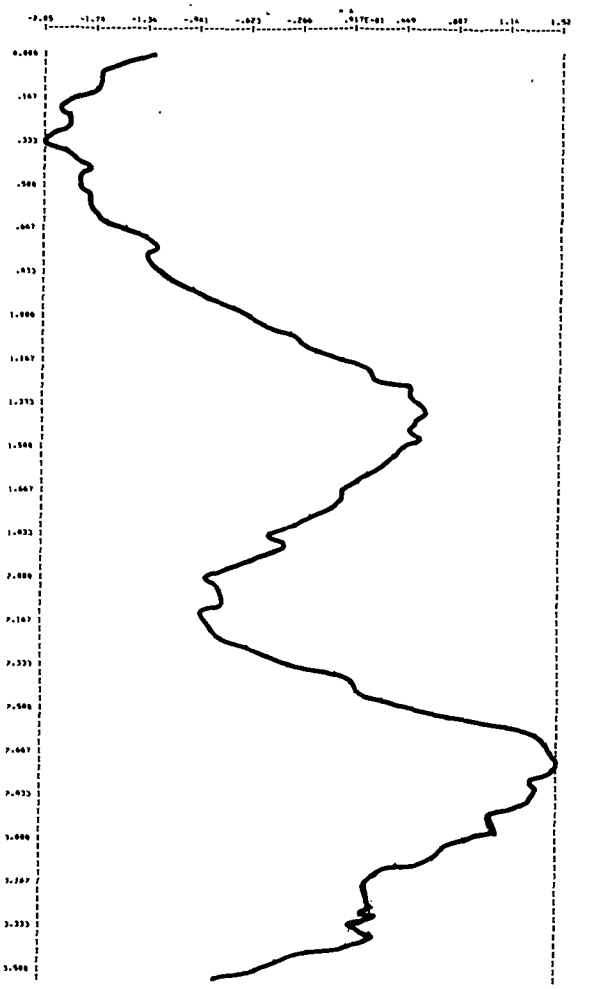

b) Generated Stick Position

Figure 18. ADI Dwell 3

STICK POSITION

TIME
(SECS)

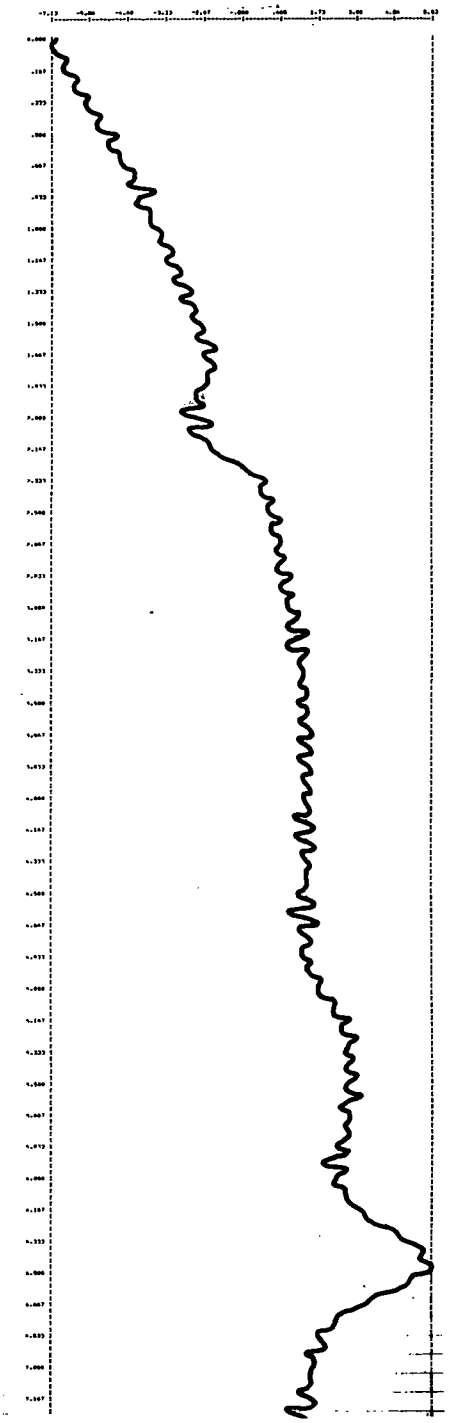

a) Actual Stick Position

Figure 19. ADI Dwell 4

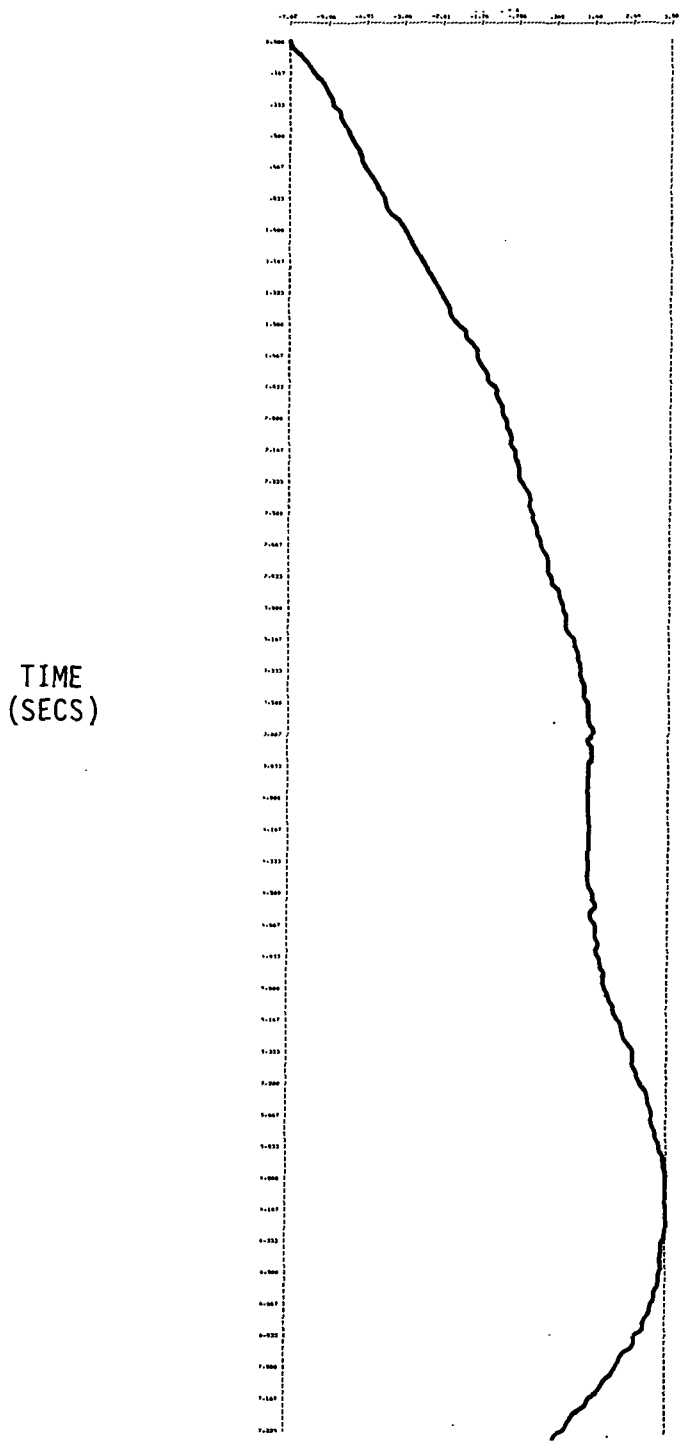

b) Generated Stick Position

Figure 19. ADI Dwell 4

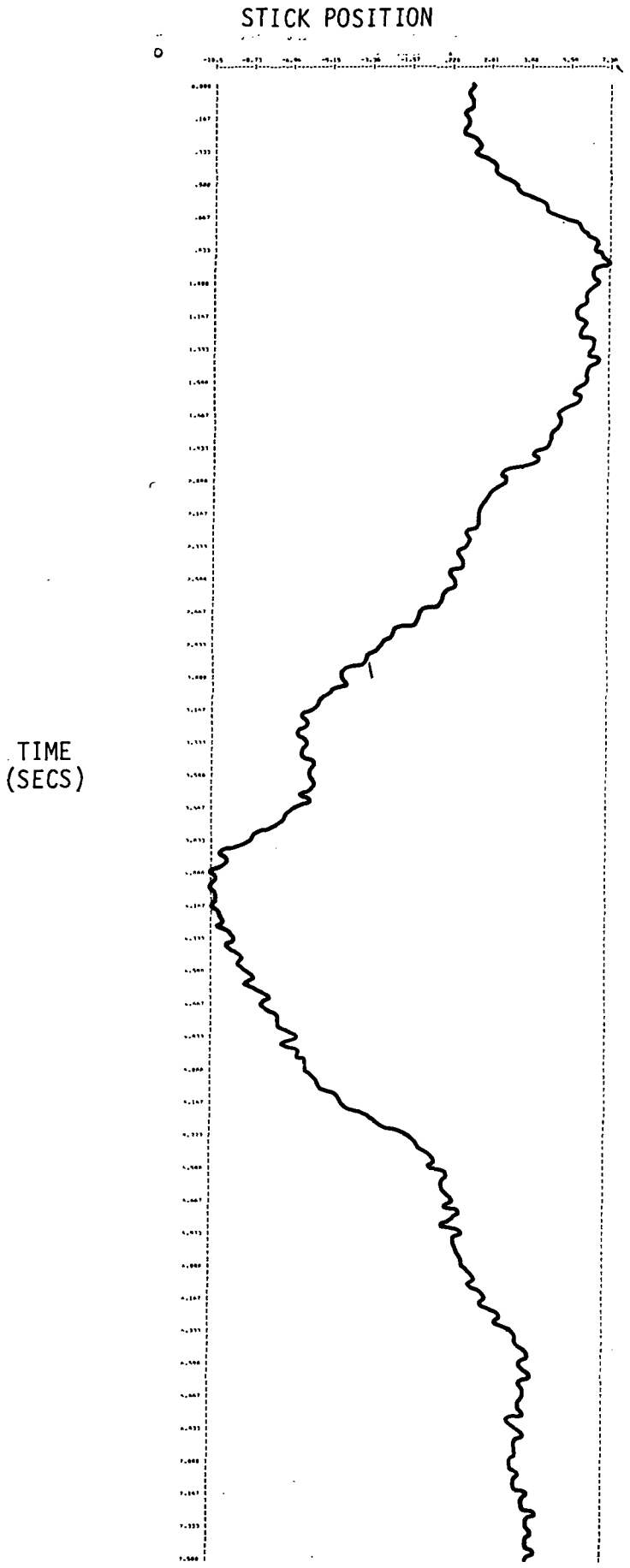

a) Actual Stick Position

Figure 20. ADI Dwell 5

STICK POSITION

TIME
(SECS)

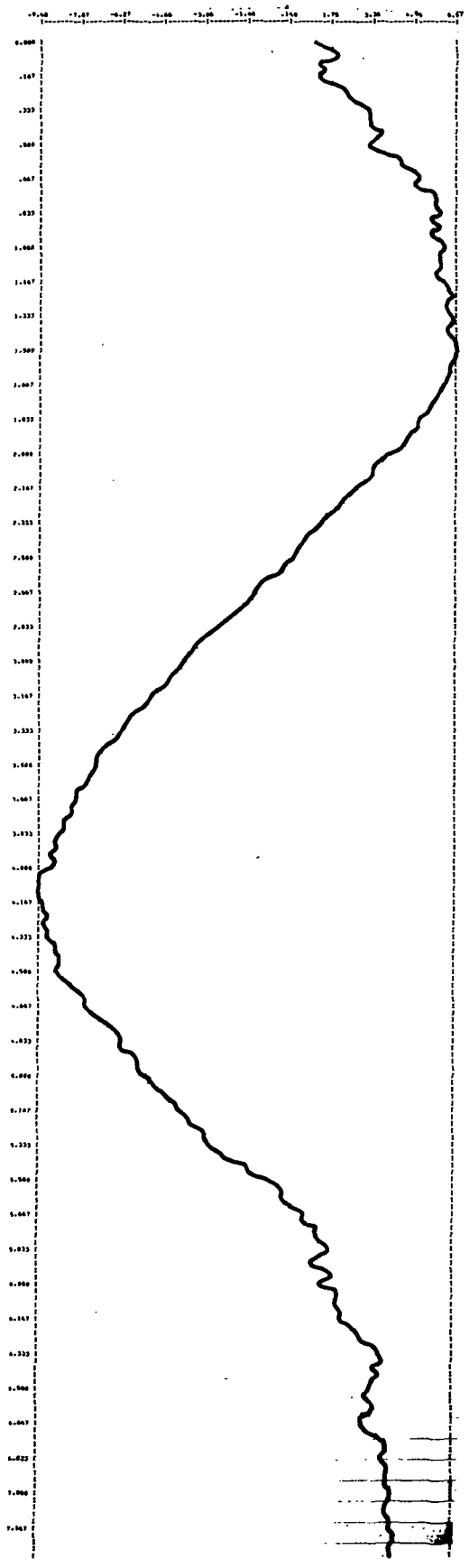

b) Generated Stick Position

Figure 20. ADI Dwell 5

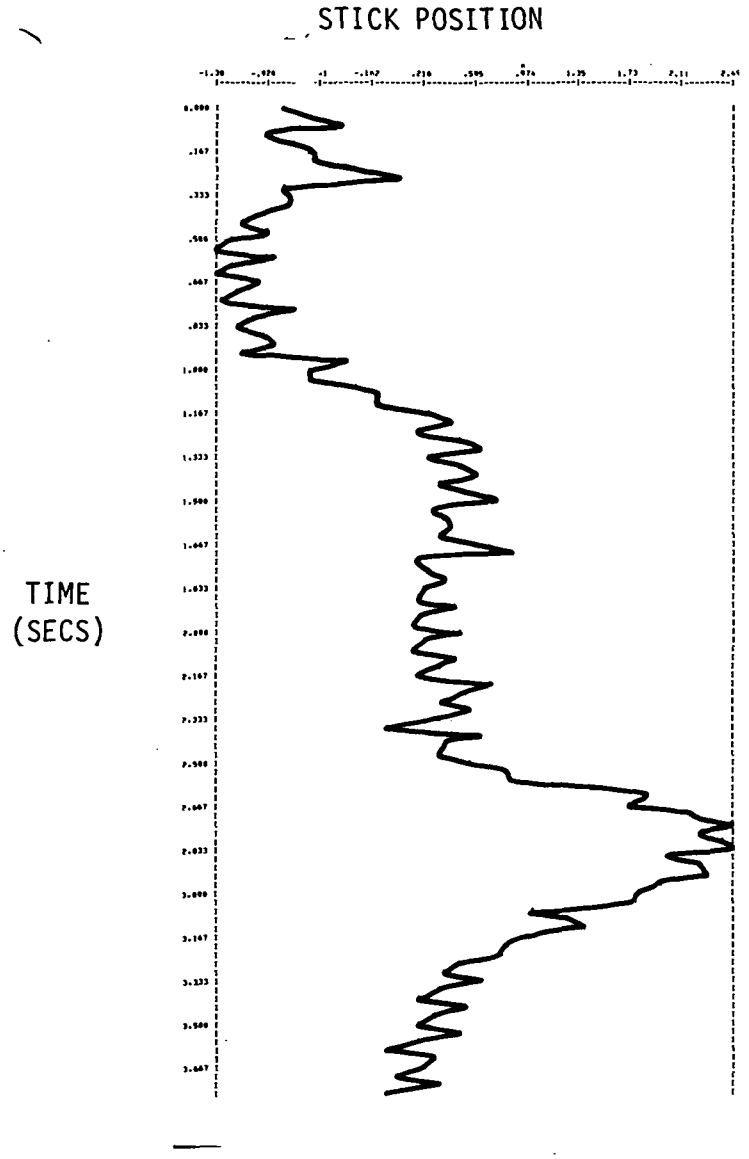

a) Actual Stick Position

Figure 21. ADI Dwell 6

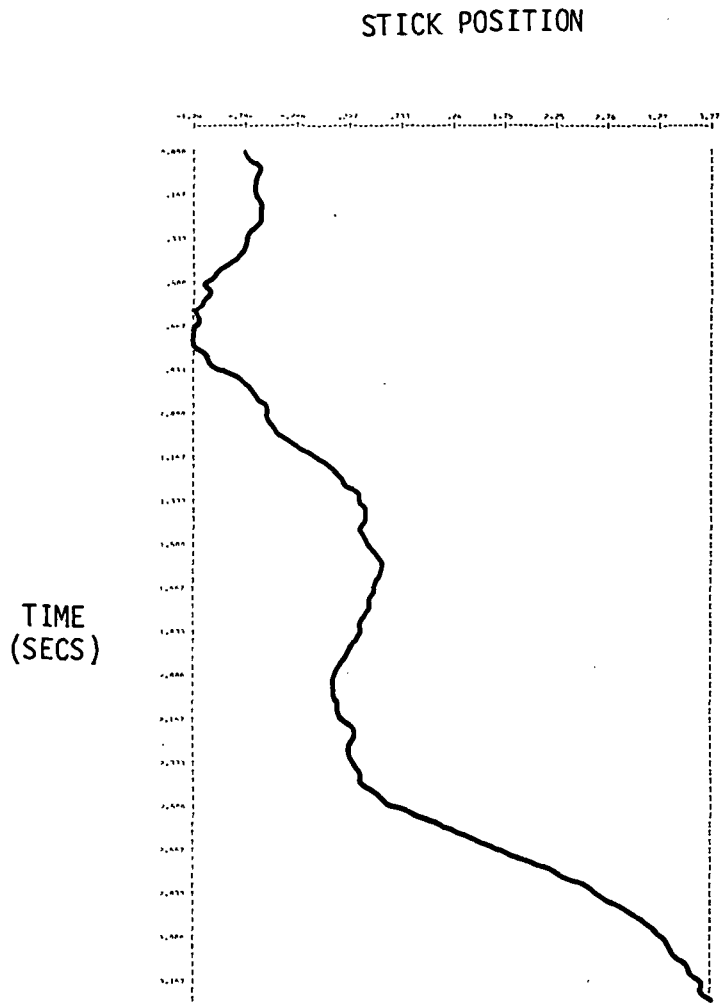

b) Generated Stick Position

Figure 21. ADI Dwell 6

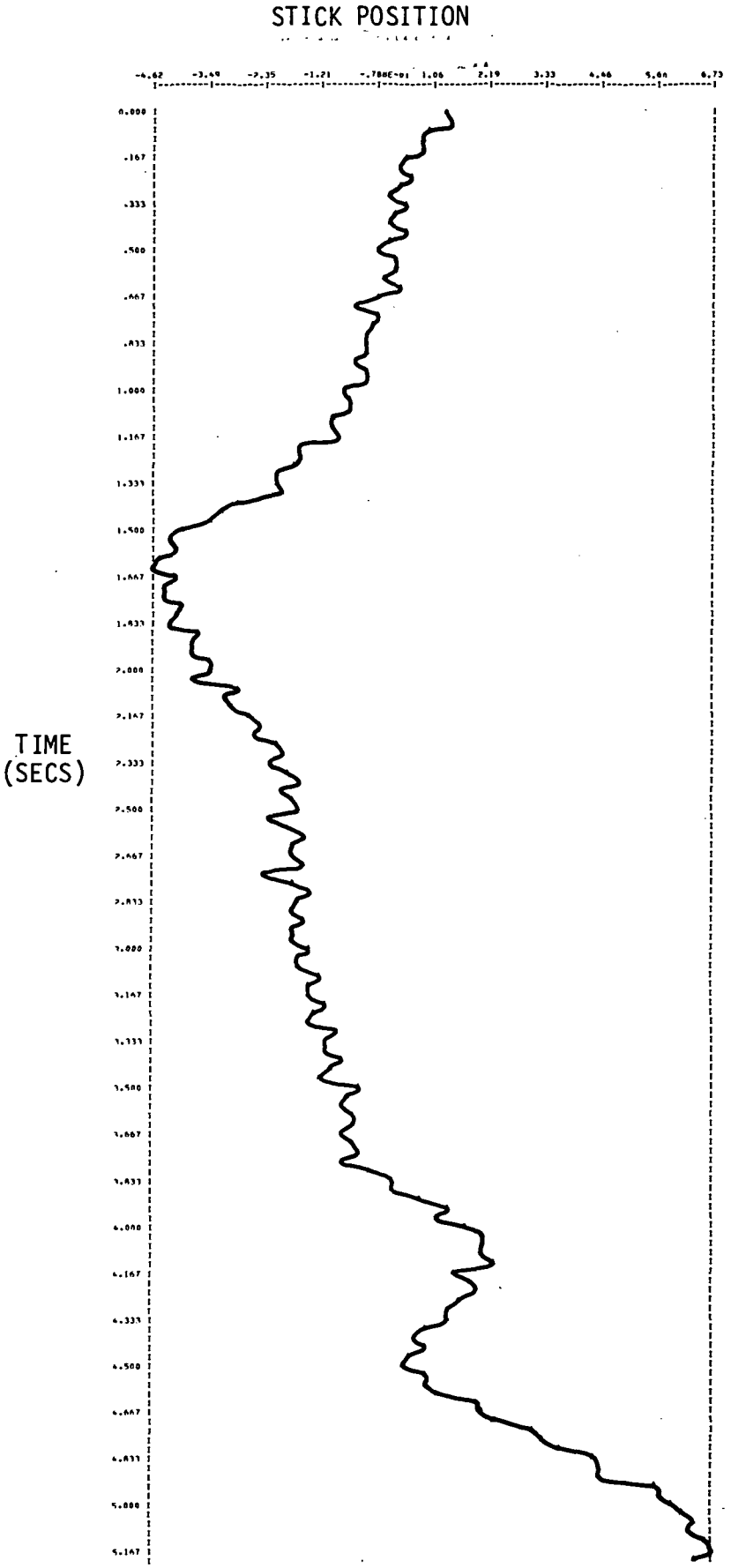

a) Actual Stick Position

Figure 22. ADI Dwell 7

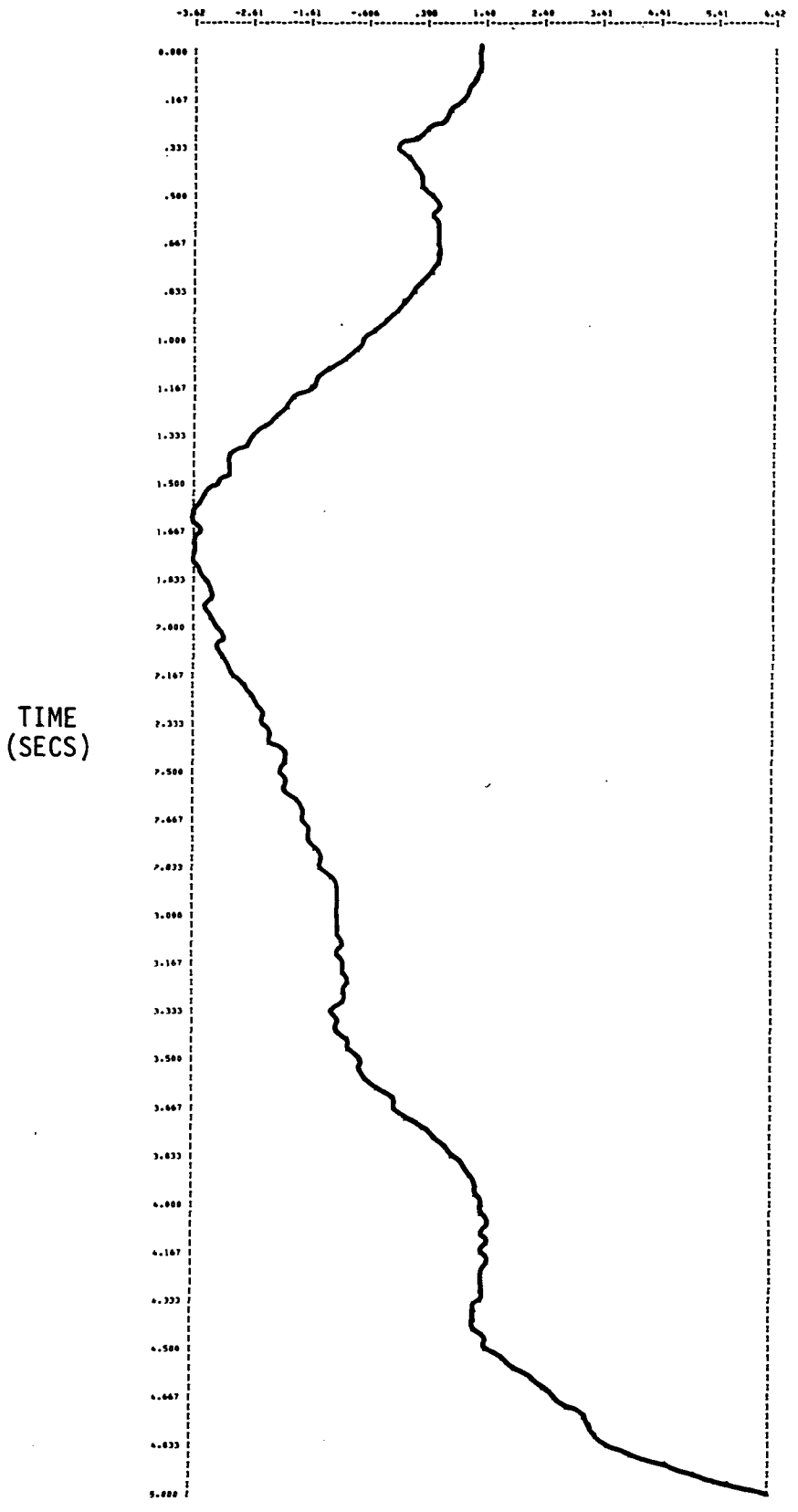

b) Generated Stick Position

Figure 22. ADI Dwell 7

SECTION VI

CONCLUSIONS AND RECOMMENDATIONS

The overall objective of the study was to develop a preliminary model of workload comprised of eye behavior variables. To do this, rate of change of the state variables was assumed to be the best indication of the ordering of the flight conditions in terms of task difficulty. Eye data were then examined to determine how changes in the various vision-related variables reflected this difficulty.

The primary tool used in the development of the model was stepwise linear regression. At a general level of analysis, pupil diameter was shown to have a strong relationship to pilot workload. This was not found when the data were examined in more detail using individual runs for individual subjects. It was concluded that the pupil diameter measure as used initially was most likely not a pure measure but rather a composite score reflecting both pupil dilation and instrument scanning activities. If this is in fact true, it does not diminish the value of the obtained relationship.

Extensive analysis of dwell time on specific instruments showed high variability between pilots and within a given pilot over several runs. No significant relationship between instrument dwell time and pilot workload was found. This was somewhat unexpected.

Recommendations for future research include the examination of the pupil diameter variable from other data sets such as those being obtained at the

Langley Research Center, Simulation and Human Factors Branch. Dwell time data should be similarly explored. It is recommended that emphasis by placed on examining more extensive data from perhaps fewer pilots. No consistent "strategy" was apparent over several runs under equivalent conditions. If such a strategy exists, it may become more apparent as more data are examined.

While the present study included what was felt to be a reasonable range of task difficulty, it might be of value to explore a greater range of conditions, particularly at higher levels of pilot workload. It may be found that certain relationships appear only under the more extreme conditions.

The use of maximum likelihood techniques to identify dominant pilot system variable inputs, such as variables of primary importance to the given pilot task, proved successful. Furthermore, positive indications of the ability of the horizontal steering pointer to provide this information were obtained. This is because fixations on the ADI could be isolated by using the oculometer output.

On the other hand, the MLE results proved somewhat disappointing with regard to the original analysis goals. The MLE process did not isolate the display variable of concentration. For example, HSP fixations would be expected to produce higher dominance of this display variable in the identification. This was not the case as other variables, usually more closely related the actual control task, tended to dominate the pilot parameter reconstruction.

Recommendations for expansion of this technique are as follows:

1. A more precise definition of the dynamic characteristics of the pilot could be obtained by incorporating several modifications to the analysis process.
   a) Only a single display variable should be used in the identification process. In the present case, only the horizontal steering pointer should be used. This would eliminate gain identification on other display variables resulting in computation reduction and would lead to expansion of pilot model structure.
   b) Since the horizontal steering pointer is a display design variable, that is, frequency-shaped combination of plant-states, the design process can be optimized by examining pilot parameters associated with various designs. These parameters can be evaluated for pilot acceptability.
   c) A better way of normalizing display variables should be provided. This will produce easier interpretation of pilot parameters. The scaling used here produced some large parameter magnitude differences.
2. Pilot parameters correlated well with pilot ratings under ideal circumstances. Under real world flying conditions, the oculometer is an effective tool for isolating specific periods for close examination.
3. Finally, it should be recognized that this MLE effort was very limited in scope. Analysis of more samples representing a variety of flight segments and task difficulty should be considered.

SECTION VII

REFERENCES

1. Baron, S., et al., "Application of Optimal Control Theory to the Prediction of Human Performance in a Complex Task," AFFDL TR-69-81, March 1970.

2. Bradshaw, J. L., "Load and Pupillary Changes in Continuous Processing Tasks," British Journal of Psychology, 1968, 59, 265-271.

3. Hess, E. H. and Polt, J. M., "Pupil Size in Relation to Mental Activity during Simple Problem Solving," Science, 1964, 143, 1190-1192.

4. McRuer, D. T. and Krendel, E. S., "Dynamic Response of Human Operations," Wright Air Development Center, Wright-Patterson AFB, Ohio, WADC TR56-524, October 1957.

5. Myers, J. L., Fundamentals of Experimental Design, Boston, Allyn and Bacon Inc., 1966.

6. Payne, D. T., Parry, M. E., and Harasymiw, S. J., "Percentage of Pupillary Dilation as a Measure of Item Difficulty," Perception and Psychophysics, 1968, 4, 139-143.

7. Phatak, A., "Identification of the Optimal Control Model for the Human Operator," AMRL-TR-74-79, May 1975.

8. Simpson, H. M. and Hale, S. M., "Pupillary Changes during a Decision Making Task," Perceptual and Motor Skills, 1969, 29, 495-498.

9. Tse, Edison, "Information Matrix and Local Identifiability of Parameters," JACC, Columbus, Ohio, 1973.

10. Hartmann, G.L., Harvey, C.A., and Stein, G., Digital Adaptive F-8C Control Laws. Final Report, NAS1-13358, July 1975.

APPENDIX A

SIMULATION OF THE BOEING 737 A/C IN THE SIGMA FIVE HYBRID SYSTEM

SUMMARY

This section summarizes the 737 A/C simulation operational in the XDS Sigma Five Computer. The simulation was configured for approach and landing (i.e., Mach < 0.35, altitude < 1524 meters) and included the nonlinear A/C coefficients associated with large attack and flap angles. The simulation made use of the General Purpose A/C Simulation System (GPASS) using the THRUST format developed by Honeywell.

The six degree-of-freedom software package (GPASS) was used in the development of the hybrid simulation for this study. The mass aerodynamic and inertial parameters of the Boeing 737 twin jet airliner were used. Aircraft coefficients were evaluated for high attack angle conditions where Mach and altitude were less than 0.35 and 1524 meters, respectively since the flight segments to be studied were terminal approach and landing.

An Instrument Landing System (ILS) simulation was used which computed angular error signals from ILS beam centers along its reference axes to aircraft position. This angular error set was transformed to a rectangular set so that errors had the units of feet rather than degrees. The computation was:

$$\epsilon_{EL} = R \sin (GS)$$

where

ϵ_{EL} is elevation error above or below glide slope, in meters,

R is range from transmitter, in meters

GS is angular glide slope error, in degrees

$$\epsilon_{AZ} = R \sin (LOC)$$

where

ϵ_{AZ} is azimuth error to the right of runway centerline, in meters

R is range from transmitter, in meters

LOC is angular localizer error, in degrees

This avoids the problem of great increases in the sensitivity of the angular signals during the final approach phase when range to touchdown approaches small values. This is an alternate to course softening which uses a variable gain on the error signals as altitude values decrease near touchdown.

The glide slope and localizer error signals were displayed to the pilot as raw data. The elevation and azimuth error signals were used in the guidance calculations of the command/steering signals to the flight director. The stabilization portion of the command/steering signals used compensated vehicle attitude terms.

The command laws used for the steering bars were

$$HSP = -1.5 \left[0.18\, \epsilon_{EL} \frac{5.0\,S+1}{0.5\,S+1} + \frac{\theta\,(S)}{3\,S+1} + \theta_o\right]$$

where

HSP is the Horizontal Steering Pointer signal to the ADI (scale factor at 0.0254 cm/Volt),

ϵ_{EL} is the glide slope error, in meters,

S is the LaPlace operator,

θ is the aircraft pitch attitude, in degrees

θ_o is pitch bias

$$VSP = -1.0\ [0.30\ \epsilon_{AZ}\ \frac{5.0\ S+1}{0.5\ S+1}\ - 0.5\ \phi]$$

where

VSP is the Vertical Steering Pointer signal to the ADI (scale factor at 0.0254 cm/Volt)

ϵ_{AZ} is the localizer error, in meters

ϕ is aircraft roll attitude, in degrees

A speed command was developed and displayed to the pilots on a speed bug on the left side of the ADI. The commands were:

V_c = 200 knots constant, $R > 12000$

V_c = 0.0038 R knots, $12000 > R > 6000$

V_f = 120 knots, $R < 6000$ to touchdown

During the approach it was possible to fly out of the glide slope beam. The system logic placed the horizontal steering pointer in the stow position when this occurred.

A flare command was developed to drive the HSP rather than glide slope error at the terminal end of the final approach. At altitude equal to flare was initiated through a 2.5 second fader at the same time ILS was faded out. The flare command was

$$HSP = H + 6\dot{h}$$

where

h is aircraft altitude, in meters

$\dot{h}$ is descent rate, meters per second

SIMULATION DESCRIPTION

Basic mass aerodynamic and inertial parameters of the Boeing 737 are shown in Table A-1. Figure A-1 is a three-sided view of the aircraft. Longitudinal control is through the elevators and horizontal stabilizer. The stabilizer is primarily used for trim, while the elevators, mounted on the aft end of the stabilizer, are used for maneuvering and damping. Lateral control is achieved through use of ailerons, spoilers, and rudder. The spoilers are used both for assisting the ailerons and providing speed braking.

Additional surfaces are available for high-lift conditions. These surfaces are trailing and leading edge flaps as well as leading edge slots. Characteristics of all the above mentioned surfaces are discussed in more detail in Section VII. The project for which this simulation was developed had as its purpose to evaluate pilot workload during approach and landing. Hence A/C coefficients were evaluated for high attack-angle conditions.

TABLE A-1. SUMMARY OF AREAS AND DIMENSIONS

Symbol	Item	Value	Dimension
S	Wing area	91.04	m^2
$\bar{c}$	Wing mean aerodynamic chord	3.41	m
b	Wing span	28.35	m
	Effective engine moment arms about c.g.		
Y_E	Lateral arm	4.94	m
Z_E	Vertical arm	1.52	m
	Wheel base	10.46	m
	Wheel tread		
	Main gear to $\bar{c}$ point	0.98	m
	Mass (weight)	2797 slugs	
	I_{XX}	$3.75 \cdot 10^5$ slug	
	I_{YY}	$8.75 \cdot 10^5$ slug	
	I_{ZZ}	$1.20 \cdot 10^6$ slug	
	I_{XZ}	$4.80 \cdot 10^4$ slugs	
	$I_{XY} = I_{YZ} = 0$		

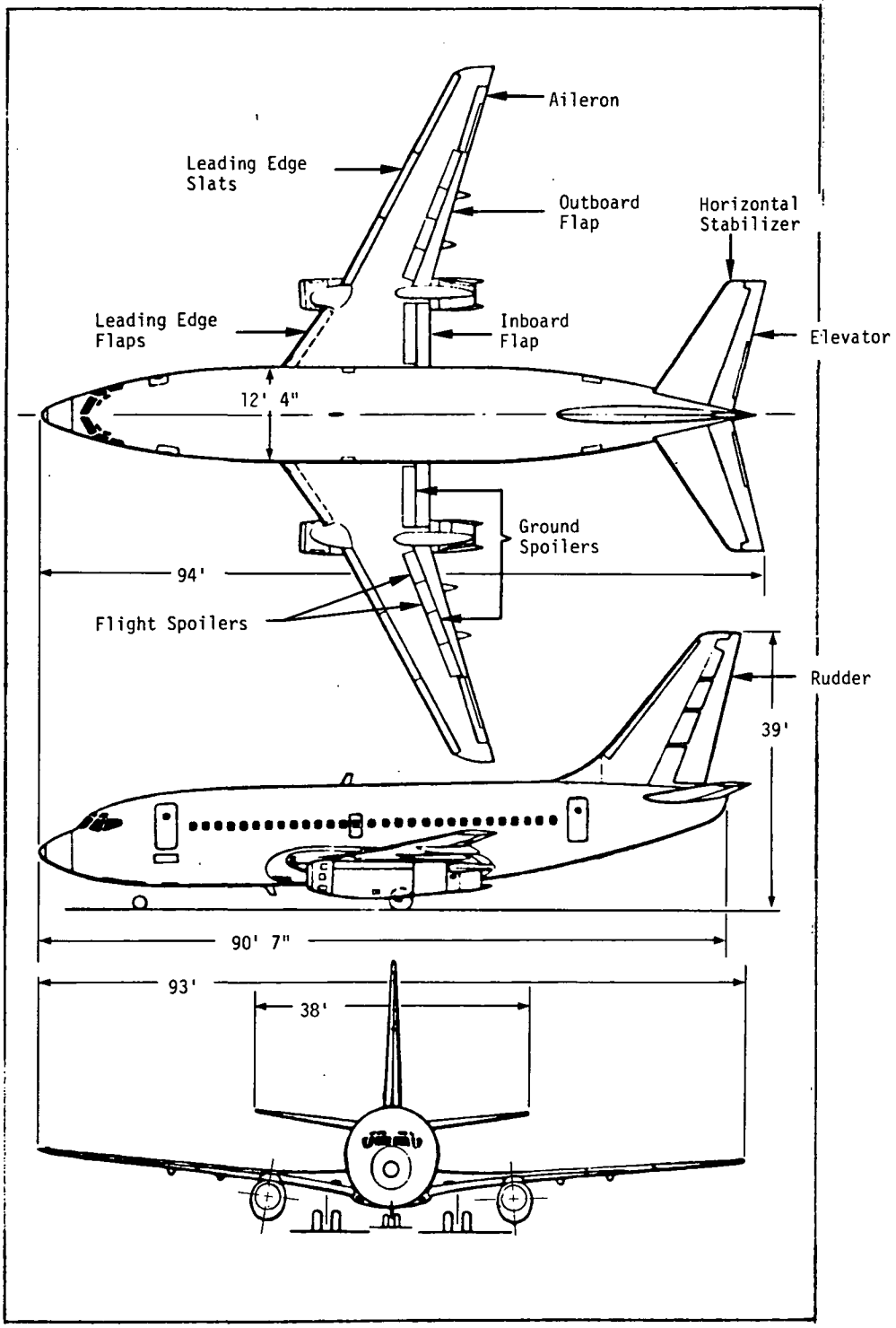

Figure A-1. Three-Sided View of the Boeing 737

Figure A-2 is a functional block diagram illustrating the operation of the control system. Manual/SAS interaction is fairly standard with the exception that a portion of the elevator position is a function of stabilizer trim position.

Figure A-3 is a listing of the aerodynamic routine, illustrating the aero dimensionless coefficients used in the simulations, as well as their method of calculation. Since the flaps have a strong effect during landing, the aero coefficients are sensitive to flap position.

The simulation is connected to the cockpit simulator via the trunk interconnect rack. Figure A-4 is a schematic of the cockpit controls and hybrid link. Included are pitch, roll, rudder pedals, throttles, spoiler, and flap control. Figure A-5 is a schematic of the cockpit instruments, driven from the hybrid link. These instruments include a flight director and ILS command needles, compass, altimeter, attitude rate, engine thrust and flap angle, and indicated airspeed.

Scale factors for the flight director and compass are 1.8° per volt (180° = 100 V). Altitude rate, attitude, and indicated airspeed are given by the following equations:

$$\dot{h}(v) = 2.7 + 0.0396 \cdot \dot{h}(m/sec) \cdot \left(\frac{1}{S+1}\right)$$

$$IAS(V) = 3.25 - 0.0165 \cdot V_{CAS}(knots) + 9 \cdot V^2_{CAS}(knots)$$

h(course/fine)

$$h_c = 2.3 + 0.0004 \cdot h(m)$$

$$h_f = -96 + 0.045 \cdot h(m)$$

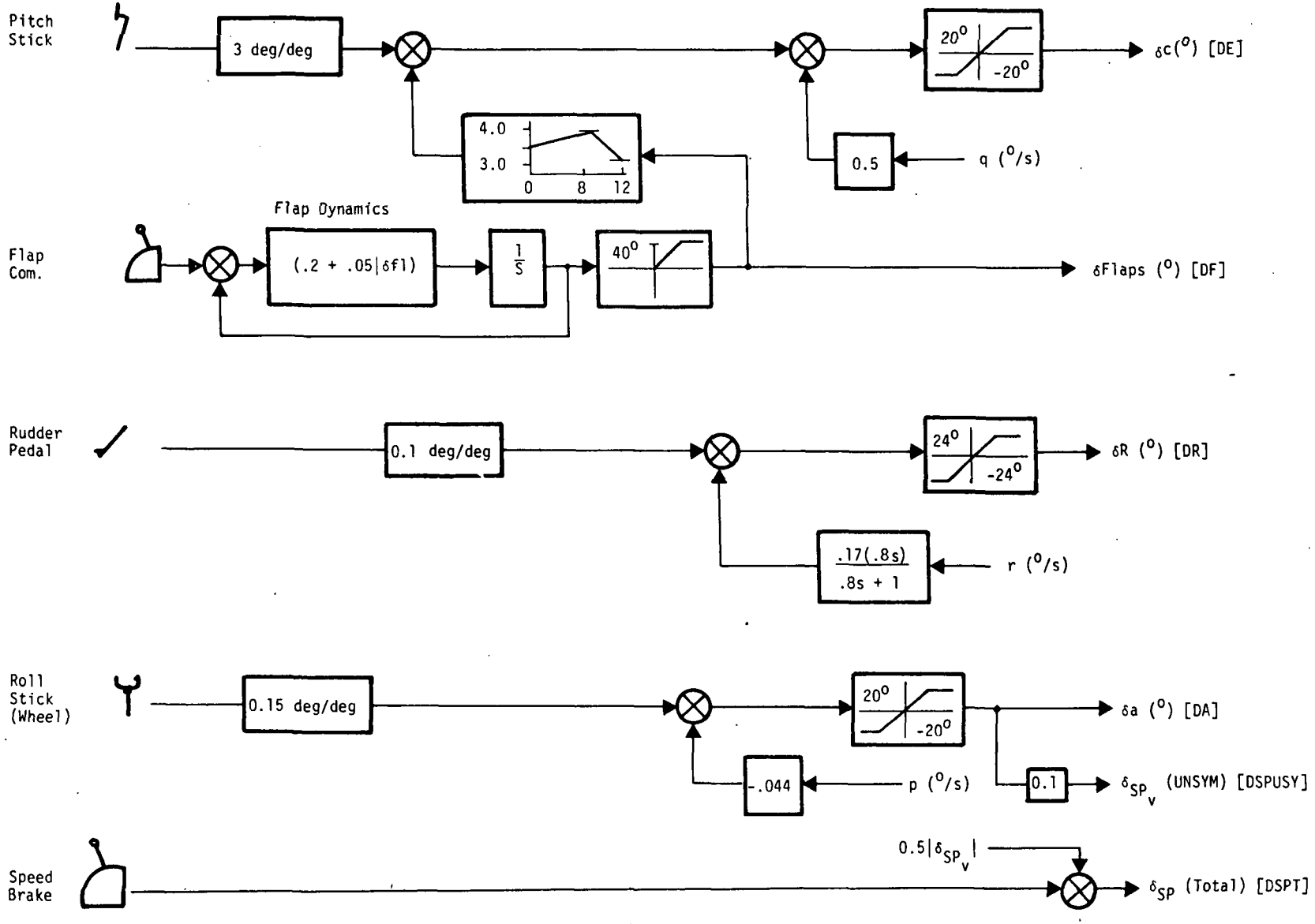

Figure A-2. Functional Block Diagram of Control System

```
C
C
      SUBROUTINE AERO
      COMMON/THRUST/MODE,A(1000)
      REAL MASS,MACH,L,M,N,LT,LW,MW,NW
      REAL IX,IY,IZ,IXZ
C
C                    **** PARAMETER INPUTS ****
C
      EQUIVALENCE (SOS   ,A(006)),(GAM   ,A(028)),(G     ,A(090)),
     1            (MASS  ,A(091)),(DXT   ,A(092)),(DZT   ,A(093)),
     2            (TX    ,A(111)),(TZ    ,A(112)),
     3            (B     ,A(115)),(C     ,A(116)),(S     ,A(117)),
     *            (CLFB  ,A(351)),(CLFADT,A(352)),(CLFO  ,A(353)),
     *            (CLFDS ,A(354)),(CLFDE ,A(355)),(CLFGSP,A(356)),
     *            (CLFFSP,A(357)),(CLFGEF,A(358)),
     *            (CDB   ,A(361)),(CDMSP ,A(362)),(CDGSP ,A(363)),
     *            (CDLG  ,A(364)),(CDGEF ,A(365)),(CDBET ,A(366)),
     *            (CDDR  ,A(367)),
     *            (CMB   ,A(371)),(CMALDT,A(372)),(CMQ   ,A(373)),
     *            (CMZ   ,A(374)),(CMDS  ,A(375)),(CMDF  ,A(376)),
     *            (CMFSP ,A(377)),(CMGSP ,A(378)),(CMLG  ,A(379)),
     *            (CMGEF ,A(380)),(CMBET ,A(381)),(CMDR  ,A(382)),
     *            (CYB   ,A(391)),(CYP   ,A(392)),(CYR   ,A(393)),
     *            (CYDSP ,A(394)),(CYDA  ,A(395)),(CYDR  ,A(396)),
     *            (CLBET ,A(401)),(CLP   ,A(402)),(CLR   ,A(403)),
     *            (CLDSP ,A(404)),(CLDA  ,A(405)),(CLDR  ,A(406)),
     *            (CNBET ,A(411)),(CNBETD,A(412)),(CNR   ,A(413)),
     *            (CNP   ,A(414)),(CNDSP ,A(415)),(CNDA  ,A(416)),
     *            (CNDR  ,A(417))
      EQUIVALENCE (TEF   ,A(420)),(FG    ,A(421)),(FGE   ,A(422)),
     *            (CLBCBR,A(423)),(CNBCBR,A(424)),
     *            (TXZ   ,A(426)),
     *            (TS    ,A(427)),(TS1   ,A(428)),(ALW   ,A(027))
C
C                    **** VARIABLE INPUTS ****
C
      EQUIVALENCE (MACH  ,A(005)),(VEL   ,A(016)),(AL    ,A(029)),
     1            (BET   ,A(030)),(ALDT  ,A(037)),(BETDT ,A(038)),
     2            (P     ,A(042)),(Q     ,A(043)),(R     ,A(044)),
     3            (DS    ,A(121)),(DE    ,A(122)),(DSPUSY,A(104)),
     4            (DA    ,A(124)),(DR    ,A(125)),(H     ,A(004)),
     5            (TC    ,A(429)),(DF    ,A(105)),(DSPT  ,A(107))
C
C                    **** VARIABLE OUTPUTS ****
C
      EQUIVALENCE (QBAR  ,A(070)),(FX    ,A(071)),(FY    ,A(072)),
     1            (FZ    ,A(073)),(L     ,A(077)),(M     ,A(078)),
     2            (N     ,A(079)),(TH    ,A(031)),(U     ,A(007)),
     3            (W     ,A(009)),(RHO   ,A(114)),(IX    ,A(083)),
     4            (IY    ,A(084)),(IZ    ,A(085)),
     5            (EAS   ,A(126)),(CAS   ,A(127))
      IF (MODE) 100,200,500
  100 IF (MODE+LE.-2) RETURN
C     *********
      DSP    = 0.
C     *********
```

Figure A-3. Listing of the Aerodynamic Routine

```
      RHOSL  = 0.00237
      B      = 93.
      SOS    = 1096.0
      C      = 11.2
      S      = 980.
      BR     = 1./145450.
      TS     = 256.5
      TS1    = .5*27
      G      = 32.2
      MASS   = 2797.2
      IX     = 375000.
      IY     = 875000.
      IZ     = 1200000.
      IXZ    = 48000.
      EFF    = 1.0
      ALW    = 0.06
      RETURN
  200 CD2    = C*0.5
      BD2    = B*0.5
      LT     = DZT*TX - DXT*TZ
      IF (MACH.EQ.0.0) MACH = VEL/SOS
      IF (VEL.EQ.0.0) VEL = MACH*SOS
      ARC    = S/(B*B*3.1416*EFF)
      CMZ    = 0.0
      IFLG   = 1
      GO TO 500
  250 CONTINUE
      CZZ    = CZAL*ALW
      TH     = GAM + AL
      STH    = SIN(TH)
      CTH    = COS(TH)
      SAL    = SIN(AL)
      CAL    = COS(AL)
      W      = VEL*SAL
      U      = VEL*CAL
      IFLG   = 0
  500 VINV   = 1.0/VEL
      SIG    = (1. - H*BR)**4.26
      RHO    = RHOSL*SIG
      CD2V   = CD2*VINV
      BD2V   = BD2*VINV
      QBAR   = 0.5*RHO*VEL*VEL
      QBARS  = QBAR*S
C
C                    COMPUTE EQUIVALENT AND CAL. AIRSPEED
C
      EAS    = VEL*SQRT(SIG)
      CAS    = VEL*(1. - 0.00004*H)
C
      IF (IFLG.EQ.1) GO TO 250
      QBARSC = QBARS*C
      QBARSB = QBARS*B
      ALD    = 57.3*AL
      BETD   = 57.3*BET
C
C                    COMPUTE STALL POINT
C
      STALPT = ALD - 10. - 0.15*DF
```

Figure A-3. Listing of the Aerodynamic Routine (Continued)

```
      CNDR    =-0.03
C
C                     SIDE FORCE COEF.
C
      CYB     =-0.022 - 0.0002*DF*(1. - 0.067*ALD)
      CYP     =-0.3 + 0.04*ALD + 0.0140*DF
      CYR     = 0.55 - 0.0063*DF*(1. + 0.060*ALD)
      CYDSP   = -0.0009*DF - 0.001*ALD
      CYDA    = 0.007 - 0.00015*DF - 0.0002*ALD
      CYDR    = 0.007
C
C                     AUXILLARY FUNCTION COEF.
C
      TEF     = 1. - 0.2*STALPT
      FG      = 1. + (0.15 -0.015*ALD + .005*DF)*EXP(-0.04*H)
      FGE     = EXP(-0.067*H)
      CLBCOR  = 1.0 + 0.2*EXP(-0.03*H)
      CNBCOR  = 1.0 - 0.15*EXP(-0.03*H)
C
C                     SUM AERO COEF.
C
      CLF     = CLB + CD2V*(CLPDT*ALDT + CLPQ*Q) + CLPNZ*0. +
     *  TEF*(CLPDS*(3.-DS) + CLPDE*DE) + FG*CLPFSP*DSPT +
     *  CLPGEF*FGE
C
      CD      = CD0 + FG*CDFSP*DSPT + CDLG
C
      CM      = CM0 + CD2V*(CMALDT*ALDT + CMQ*Q) + CMZ*1. +
     *  TEF*(CMDS*(3.-DS) + CMDE*DE) + FG*(CMFSP*DSPT) +
     *  CMLG + CMGEF*FGE + CMBET + CMDR*DR
      CL      = (CLBET - 0.00054)*BETD*CLBCOR + BD2V*(CLP*P + CLR*R) +
     *  FG*(CLDSP*DSPUSY + CLDA*DA) + CLDR*DR
C
      CN      = CNBCOR*CNBET*BETD + BD2V*(CNBET*BET + CNP*P + CNR*R) +
     *  FG*(CNDSP*DSPUSY + CNDA*DA) + CNDR*DR
C
      CY      = CYB*BETD + BD2V*(CYP*P + CYR*R) +
     *  FG*(CYDSP*DSPUSY + CLDA*DA) + CLDR*DR
C
C                     COMPUTE AERO FORCES AND MOMENTS
C
      FXW     =-QBARS*CD
      FZW     =-QBARS*CLF
      LW      = QBARSB*CL
      NW      = QBARSB*CN
      ALSQ    = AL*AL
      SAL     = AL - AL*ALSQ/6.0
      CAL     = 1.0 - 0.5*ALSQ
      FX      = CAL*FXW - SAL*FZW
      FY      = QBARS*CY
      FZ      = SAL*FXW + CAL*FZW
      L       = CAL*LW+SAL*NW
      M       = QBARSC*CM
      N       = SAL*LW + CAL*NW
      RETURN
      END
```

Figure A-3. Listing of the Aerodynamic Routine (Concluded)

```
      IF (STALPT.LE.0.0) STALPT = 0.
C
C                     COMPUTE LIFT COEF
C
      CLFB    = 0.1 + 0.11*ALD + 0.03*DF - 0.008*STALPT*STALPT
      CLFADT  = .8
      CLFQ    = 8.
      CLFDS   = 0.017
      CLFDE   = 0.008
      CLFFSP  = -0.1 - 0.006*DF
      CLFGSP  = -0.35 + 0.0205*ALD - 0.0063*DF
      CLFGEF  = 0.2 - 0.0130*ALD*(1. + 0.005*DF)
C
C                     COMPUTE DRAG COEF.
C
      CDB     = 0.04 + 0.003*DF + (.0006 + .000003*DF)*(ALD+.07*DF)*
     *   (ALD+.07*DF)
      CDFSP   = 0.02 - 0.001*ALD
      CDGSP   = 0.04 - 0.003*ALD - 0.0004*DF
      CDLG    = 0.03 - 0.00038*DF - 0.0005*ALD
C
C                     COMPUTE PITCH MOMENT COEF.
C
      CMB     = 0.1 - .030*ALD + 0.0006*ALD*ALD
      IF (DF.GT.15.0) CMB = CMB - 0.01*(DF - 15.0)
      CMALDT  = -2.
      CMQ     = -25.
      CMZ     = 0.0065
      CMDS    =-0.06
      CMDE    =-0.028
      CMFSP   = 0.02 + 0.004*ALD + 0.0015*DF
      CMGSP   =-0.12 + 0.008*ALD + 0.00080*(ALD-8.)*(ALD-8.)
      CMLG    = 0.02 - 0.001*ALD - 0.0005*DF - 0.00004*ALD*DF
      CMGEF   = 0.05 - 0.01*ALD - 0.005*DF + 0.00015*ALD*DF
C
      CMGEF   = 0.1*CMGEF
C
      CMBET   = 0.0006*BETD*BETD
      CMDR    = 0.002
C
C                     COMPUTE ROLL MOMENT COEF.
C
      CLBET   = -0.003 - 0.00004*DF - 0.00015*ALD
      CLP     =-0.5 + 0.025*ALD
      CLR     = 0.05 + 0.015*ALD + 0.0063*DF
      CLDSP   = 0.02 + 0.001*ALD + 0.0013*DF
      CLDA    = 0.025 - 0.0005*ALD
      CLDR    = 0.011
C
C                     YAW MOMENT COEF.
C
      CNBET   = 0.0035 + 0.00005*ALD - .000025*ALD*(1. + .00004*DF*DF*DF)
     *   *SIN(12.*AL)
      CNBETD =-0.02 + 0.0008*ALD + 0.00006*DF*ALD
      CNP     =-0.03 + 0.0012*(ALD-10.)*(ALD-10.) - 0.0037*DF
      CNR     =-0.25 - 0.008*ALD
      CNDSP   = 0.005 - 0.00025*ALD + 0.00025*DF
      CNDA    = 0.0005 - 0.00015*ALD + 0.00005*DF
```

Figure A-3. Listing of the Aerodynamic Routine (Continued)

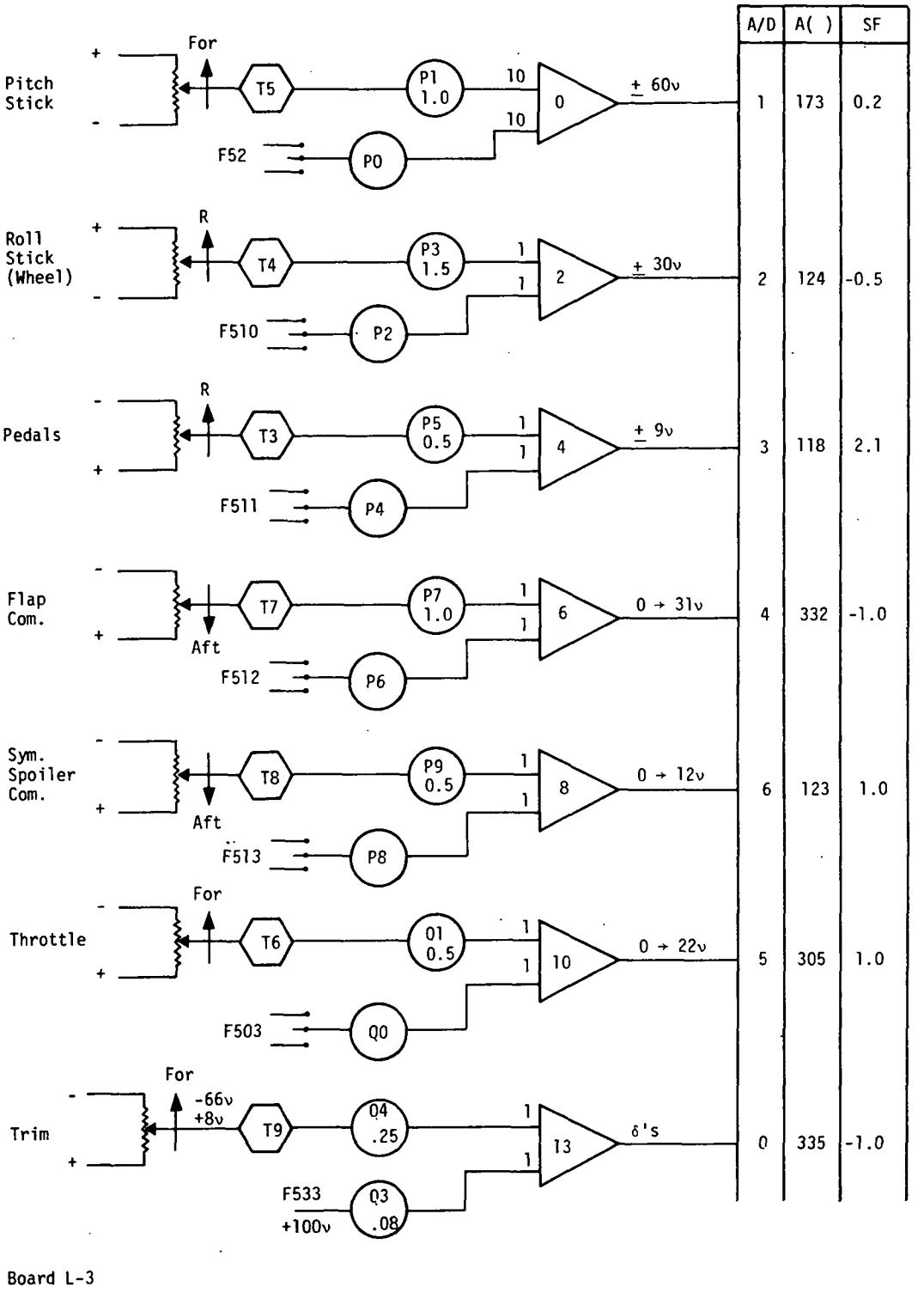

Board L-3

Figure A-4. A Schematic of the Cockpit Controls and Hybrid Link

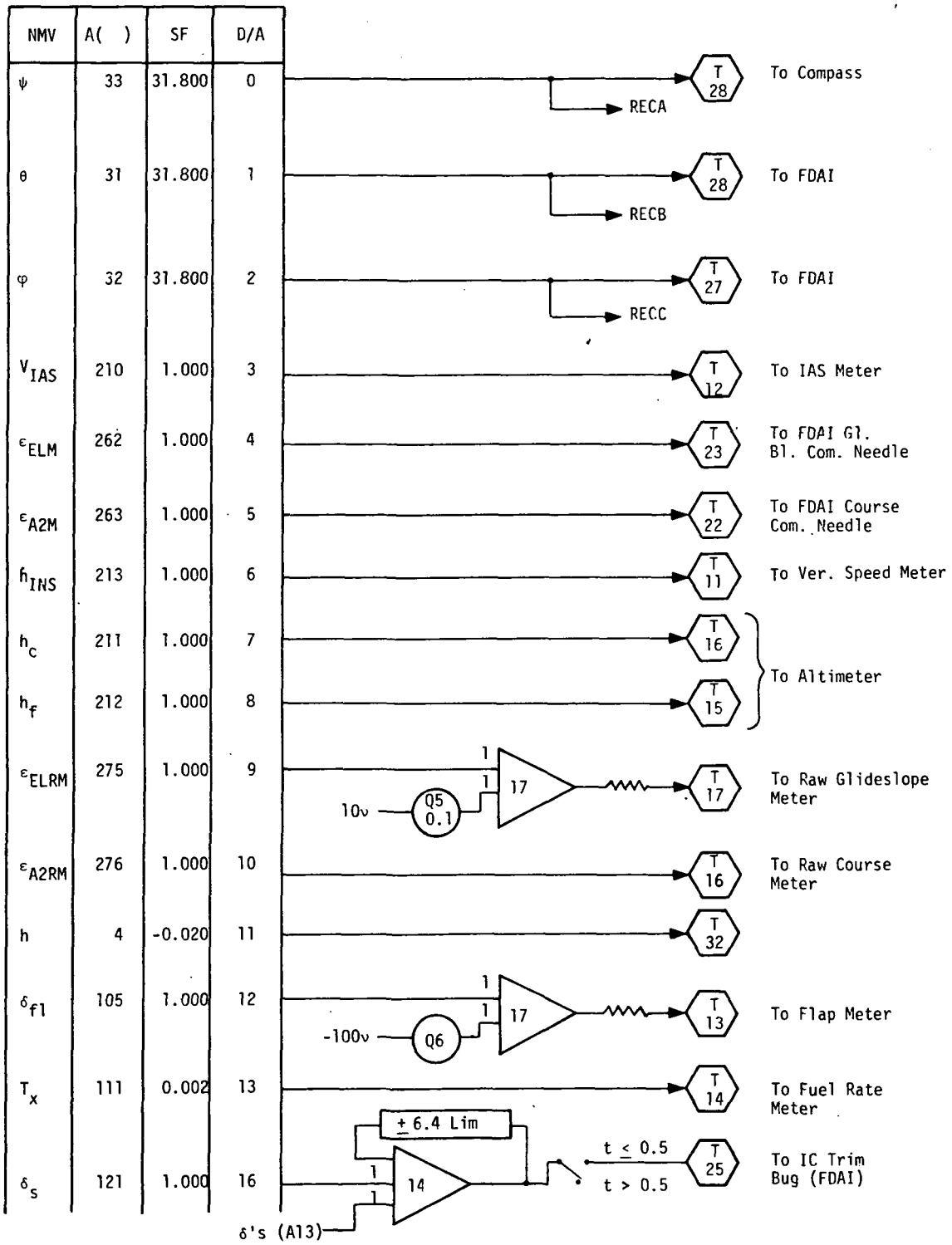

Figure A-5. A Schematic of the Cockpit Instruments, Driven from the Hybrid Link

It should be noted that the attitude instrument requires a course and fine signal; in order to get realistic vertical speed, h, is filtered with a one-second lag.

The longitudinal response to α gusts and a pilot input indicate that both free aircraft and SAS response is well damped. Predicted free aircraft response is:

$\omega_{\alpha} = 1.8$ rad/sec (3-second period)

$\zeta_{\alpha} = 0.45$

Observed period and damping ratio was about 2.8 seconds at a damping ratio of 0.4.

Response to pilot inputs for the lateral axis was improved by the SAS so that the response was well damped and maintained the command roll rate. Predicted lateral response is:

$\omega_{\beta} \approx 1.47$ rad/sec

$\zeta_{\beta} \approx 0.14$

The observed frequency and damping ratio was 1.54 rad/sec and 0.13, respectively.

APPENDIX B

THE COOPER-HARPER SCALE

CONTROLLABLE Capable of Being Controlled or Managed in Context of Mission, With Available Pilot Attention	ACCEPTABLE May Have Deficiencies Which Warrant Improvement, But Adequate for Mission. Pilot Compensation, If Required to Achieve Acceptable Performance, Is Feasible.	SATISFACTORY Meets All Requirements and Expectations. Good Enough Without Improvement Clearly Adequate for Mission	Excellent Highly Desirable	A1
			Good Pleasant Well Behaved	A2
			Fair Some Mildly Unpleasant Characteristics. Good Enough for Mission Without Improvement.	A3
		UNSATISFACTORY Reluctantly Acceptable. Deficiencies Which Warrant Improvement. Performance Adequate for Mission With Feasible Pilot Compensation.	Some Minor But Annoying Deficiencies. Improvement Is Requested. Effect On Performance Is Easily Compensated for by Pilot.	A4
			Moderately Objectionable Deficiencies. Improvement Is Needed. Reasonable Performance Requires Considerable Pilot Compensation	A5
			Very Objectionable Deficiencies. Major Improvements are Needed. Requires Best Available Pilot Compensation to Achieve Acceptable Performance.	A6
	UNACCEPTABLE Deficiencies Which Require Mandatory Improvement. Inadequate Performance For Mission Ever With Maximum Possible Pilot Compensation.		Major Deficiencies Which Require Mandatory Improvement for Acceptance. Controllable. Performance Inadequate for Mission, or Pilot Compensation Required for Minimum Acceptable Performance in Mission is Too High.	07
			Controllable With Difficulty. Requires Substantial Pilot Skill and Attention to Retain Control and Continue Mission.	08
			Marginally Controllable in Mission. Requires Maximum Available Pilot Skill and Attention to Retain Control.	09
UNCONTROLLABLE Control Will be Lost During Some Portion of Mission.			Uncontrollable in Mission.	10

APPENDIX C

MAXIMUM LIKELIHOOD ESTIMATION ANALYSIS PROCEDURE

The procedure used in the analysis reported in Section V consisted of employing Honeywell's Maximum Likelihood Estimation software package to simulation data generated during the initial phase of the Honeywell study, Use of the Oculometer in Pilot Workload Measurement. This package was developed on earlier Honeywell internal research efforts and refined under contract to NASA/Langley (Reference 10).

Basically, the identification operates on an input/output data set with some notion that the two are related dynamically. A dynamic structure is first postulated:

$$\dot{x} = f(x, t, u, c, \xi) \; ; \; x(o) = x_o$$

$$y = h(x, t, u, c) + \eta$$

where

$x(t)$ = n-dimensional state vector

c = unknown constant parameters

$\xi(t)$ = white noise process distrubance vector

$$E\left[\xi(t)\right]=0; \; E\left[\xi^T(t)\; \xi^T(\tau)\right] = Q\,\delta(t-\tau)$$

$u(t)$ = input vector

$y(t)$ = output vector

$\eta(t)$ = measurement disturbance; white noise

$$E\left[\eta(t)\right] = 0; \;\; E\left[\eta(t)\; \eta(\tau)^T\right] = R\,\delta(t-\tau)$$

Operating in a linear descrete format the model becomes

$$x_{i+1} = A(c)x_i + B_1(c)u_i + B_2(c)\xi i$$

$$y_i = C(c)x_i + u_i + \eta i$$

The goal is to identify the unknown parameter vector $\hat{c}$ which best fits the model to a measured input time sequence, u_i's, and measured output time sequence, y_i's.

MLE attacks the problem with a conditional density function

$P(a \mid b = \beta, \alpha)$ = probability density function for random variable 'a' given that random variable 'b' has a value 'β'; α is also given.

In this case

$$\hat{c} = \text{Arg}\left[\max_{\xi} P(Y_N / c = \xi, U_N)\right]$$

(Arg[max P] means the argument or variable of the P function which maximizes P.)

N = the entire collection of Y and U

$$Y_N = (y_1, y_2, \ldots, y_N)$$

$$U_N = (u_1, u_2, \ldots, u_N)$$

The interpretation is that $\xi = \hat{c}$ maximizes the probability that Y_N outputs will result from a system with U_N as the input sequence.

In usable form, the actual maximization is performed on the log likelihood function:

$$L(\xi) = \text{Ln}\ \rho(Y_N \mid c = \xi, U_N)$$

$$= 1/2\ ||c_o - \xi||^2\ P_o^{-1} - 1/2 \sum_{k=1}^{N} (\text{Ln det}\beta_k, + ||V_k||^2_{\beta_k} - 1)$$

where β_k and V_k are defined as follows:

$$v_K = y_K - \hat{y}_K$$

where y_K is the actual output measured at time (K)

$\hat{y}_K$ is the predicted output of the model with parameters ξ.

β_K is the error covariance of the residuals, $E\left[v_K v_K^t\right]$

Further mention of the Kalman filter portion of this development is deferred (Reference 9, Tse, 1973) because as we will soon see, it is not used here.

The use of the Kalman estimator assumes some knowledge of the noise characteristics Q and R (however these ~~two~~ can be identified). For the current application it was felt that these noise characteristics were not sufficiently known to either assume some Q and R or estimate them. This means that the identification proceeds without Kalman filtering, that is, no smoothing of measurements. The identification, therefore, can be reduced to a least squares on the residuals v_i.

$$\hat{c} = \text{Arg}\left\{\min_{\xi}\left[\sum_{k=1}^{N} ||v_k(\xi)||^2 \beta_k^{-1} 1\right]\right\}$$

NASA CR-145153

DISTRIBUTION LIST
NAS1-13092

	No. Copies
NASA Langley Research Center Hampton, VA 23665 Attn: Report & Manuscript Control Office, Mail Stop 180A	1
Marvin C. Waller, Mail Stop 152D	35
NASA Ames Research Center Moffett Field, CA 94035	1
Attn: Library, Mail Stop 202-3	1
NASA Dryden Flight Research Center P.O. Box 273 Edwards, CA 93523 Attn: Library	1
NASA Goddard Space Flight Center Greenbelt, MD 20771 Attn: Library	1
NASA Lyndon B. Johnson Space Center 2101 Webster Seabrook Road Houston, TX 77058 Attn: JM6/Library	1
NASA Marshall Space Flight Center Huntsville, AL 35812 Attn: Library, AS61L	1
Jet Propulsion Laboratory 4800 Oak Grove Drive Pasadena, CA 91103 Attn: Library, Mail 111-113	1
NASA Lewis Research Center 21000 Brookpark Road Cleveland, OH 44135 Attn: Library, Mail Stop 60-3	1
NASA John F. Kennedy Space Center Kennedy Space Center, FL 32899 Attn: Library, IS-DOC-1L	1
National Aeronautics & Space Administration Washington, DC 20546 Attn: RB	1
NASA Scientific & Technical Information Facility P.O. Box 8757 Baltimore/Washington International Airport Maryland 21240	30 plus original